

## **Irrigation and Drainage monitoring by remote sensing for Ecosystems and Water resources management**

*Maria José Escorihuela<sup>1</sup>, Víctor Altés Gaspar<sup>2</sup>, Giovanni Paolini<sup>1</sup>, Josep M. Villar<sup>2</sup>, Miquel Pasqua<sup>3</sup>, Pere Quintana-Seguí<sup>3</sup>, Teodosio Lacava<sup>4</sup>, Felice Albano<sup>4</sup>, Emanuele Ciancia<sup>4</sup>, Meriam Lahsaini<sup>5</sup>, Salah Er-raki<sup>6</sup> and Olivier Merlin<sup>6</sup>*

<sup>1</sup>*isardSAT, Parc Tecnològic Barcelona Activa, Carrer de Marie Curie, 8, 08042 Barcelona, Spain*

<sup>2</sup>*Environment and Soil Science Department, University of Lleida, 25003 Lleida, Spain*

<sup>3</sup>*Observatori de l'Ebre (Universitat Ramon Llull - CSIC), Roquetes, Spain*

<sup>4</sup>*Instituto di Metodologie per l'Analisi Ambientale (IMAA), Italy*

<sup>5</sup>*Université Cadi Ayyad (UCAM), Morocco*

<sup>6</sup>*Centre d'Etudes Spatiales de la Biosphère (CESBIO), France*

IDEWA proposes the development of **innovative irrigation management tools** based on readily available multi-sensor remote sensing data that will, for the first time, allow **monitoring of the water use and drainage at field and basin scales**, and their impact on downstream ecosystems. The objectives of this project are:

1. To improve our knowledge on the downstream impacts of irrigation.
2. To develop innovative algorithms to estimate high spatial resolution soil moisture, evapotranspiration, and characterize vegetation status and water quality from Earth Observation data.
3. To work together with local irrigation community to ensure bidirectional knowledge transfer.

The project has been implemented in two Mediterranean well-monitored study areas in the Ebro (Spain) and Tensift (Morocco) basins. In this presentation we will focus on the Algerri-Balaguer irrigation district which is located within the Noguera (a tributary of the Ebro river) basin. We will present the advanced remotely sensed products developed, mainly the high-resolution soil moisture and irrigation types classification as well as the analysis about the impact of the irrigation implementation in the downstream ecosystems.

The IDEWA project (ANR-19-P026-003) is part of the [Partnership for Research and Innovation in the Mediterranean Area \(PRIMA\)](#) programme supported by the European Union.

## Characterization of cereals yields using different models based on remote sensing indicators from the Sentinel-1 and Sentinel-2 images in a semi-arid region

Aicha Chahbi Belakanji<sup>1\*</sup>, Echraf Shil<sup>1</sup>, Manel Khlif<sup>1</sup>, Mehrez Zribi<sup>2</sup>, Zohra Lili Chabaane<sup>1</sup>  
<sup>1</sup> University of Carthage, National Agronomic Institute of Tunisia, LR GREEN-TEAM. 43 Avenue Charles Nicolle, Tunis 1082, Tunisia; <sup>2</sup> CESBIO, Université de Toulouse CNRS/UPS/IRD/CNES/INRAE, 18 av. Edouard Belin, bpi 2801, CEDEX 9, 31401 Toulouse, France  
[aicha.chahbi@inat.ucar.tn](mailto:aicha.chahbi@inat.ucar.tn)

**Keywords:** Crop yield forecasting, Random Forest, Regression Model, Remote Sensing Indices, Cereal.

Crop production forecasting is critical for enhancing food security, the regulation of food prices and ensuring an appropriate food supply. It is critical to complete this activity with high precision at the regional and national levels to facilitate early decision-making. Cereal is one of the crops that played a crucial role in food security, particularly South Mediterranean countries rely heavily on cereal imports to cover their domestic consumption needs. Different methodologies have been proposed over the last decades, for the early grain yield prediction using specific multi- and hyper-spectral sensors. The main objective of this study is to develop empirical models for early prediction of cereal yields at a provincial scale. The study area is located in central Tunisia (9°23' - 10°17' E, 35° 1'-35°55' N).

To achieve this goal, we built forecasting models using multisource data as predictors, including remote sensing-based indices From Sentinel-2 and Sentinel-1 images, and experimental measurements made on cereal test plots over two agriculture years (2017-2018 and 2020-2021). And to build these models, we relied on regression model and machine learning algorithms such as Random Forest (RF).

From Sentinel-2 and Sentinel-1 images, a combined index was developed based on the combination of optical index and the radar index VH/VV as studies have shown that the radar index is correlated with different stages of cereals. The regression model based on this combined index can accurately predict cereal yield in March (three months before harvest) with an  $R^2 = 0.64$  for the average seed weight and the average straw weight. The validation of the estimates obtained made with an error equal to 10.28 qx/ha and 6.84 qx/ha, respectively for the seed and straw yields.

The second approach is based on RF, we considered two sets of fields. The first of which had fifty-one fields and was used for the development of our methodology, and the second of which had also fifty-one fields and was used for its validation. This method has been tested with several indices, the use of indices using Red-Edge bands improved the model. It allows estimation in the same period as the regression model but with a better correlation especially for seed yields with  $R^2 = 0.85$ . Also, it improved the prediction performance by reducing the error by 30% (equivalent to 6.87 qx/ha). However, for straw yields the correlation is equal to 0.72 and the error is greater than the regression model (RMSE = 9.68 qx/ha).

The results show that combining data from multiple sources outperformed models based on one dataset only. In addition, satellite indices are a major source of information for an early grain forecast, more than 2 months before harvest. The RF method exhibited the best metrics for an early estimation of seed yields however regression model showed its performance for estimating straws. In conclusion, the results of this study pointed out that combining remote sensing indices using a machine learning technique is a promising approach for cereal yield forecasting.

## **Automatization of an Early Cereal Classification Model using Random Forest and Remote Sensing Data in a Semi-Arid Region**

Manel Khlif<sup>1,\*</sup>, Maria José Escorihuela<sup>2</sup>, Aicha Chahbi Bellakanji<sup>1</sup>, Giovanni Paolini<sup>2</sup>, Zeineb Kassouk<sup>1</sup> and Zohra Lili Chabaane<sup>1</sup>

<sup>1</sup> *University of Carthage, National Agronomic Institute of Tunisia, LR GREEN-TEAM. 43 Avenue Charles Nicolle, Tunis 1082, Tunisia;* <sup>2</sup> *isardSAT, Technological Park, Marie Curie, 8-14, 08042, Barcelona, Catalonia*  
[manel.khlif@inat.u-carthage.tn](mailto:manel.khlif@inat.u-carthage.tn)

**Keywords:** Multi-year classification, Early Cereal map, Random Forest, Sentinel 2, Landsat

Land use maps are useful for analyzing territorial changes and efficiently managing agricultural land. This significance is particularly pronounced in countries that are not self-sufficient and heavily rely on external sources for their agricultural needs. Early cereal mapping in the year is crucial for government decision-making, particularly with regard to food security and the food market. Therefore, the main objective of our study is to develop a multi-year classification model for mapping winter cereal. The second objective is to identify cereal extends as early as possible in the agricultural season.

To achieve this, a classification model has been calibrated for the reference agricultural year 2020/2021 using the Random Forest classifier based on vegetation indices calculated from Sentinel 2 data (S2). Subsequently, the reference classifier model was applied for previous seasons from 2011/2012 to 2021/2022, using both S2 and Landsat (7 and 8) data, and validated using field observation data taken in the same periods.

The reference classification model achieved an overall accuracy (OA) of 89.3% for all classes. The validation results of the classification model show accurate results, especially for the years based on S2 data. Cereal classification exhibited excellent precision ranging from 85.8% to 95.1% when using S2 data, while lower accuracy (41% to 91.8%) was obtained when using only Landsat data. A slight confusion between cereals and cereals growing with olive trees was observed. An early cereal classification model demonstrated accurate results in February (four months before cereal harvest), with a precision of 95.2% and an OA of 87.7%. When applied to the entire period, early cereal classification exhibited a precision ranging from 85.1% to 94.2% with S2 data, while lower to accurate precision (42.6% to 95.4%) was observed with Landsat data.

The obtained results allow early land-use mapping, up to three or four months before the cereal harvest, with a precision for cereal crops that is comparable to a map produced at the end of the cycle, without the need for field observation data. This methodology can be adapted on a large national scale and it gives a decision-support tool for food security.

## Space based disaster management: Tunisian Experience

Wafa Talhaoui\*, Thouraya Sahli Chahed

*National Center of Mapping and Remote Sensing TUNISIA*

[Wafa.talhaoui.geo@gmail.com](mailto:Wafa.talhaoui.geo@gmail.com), [cnct@defense.tn](mailto:cnct@defense.tn)

**Keywords:** Disaster management, Geospatial Information, UNSPIDER program.

Tunisia is exposed to numerous hazards and vulnerabilities. Its geology, morphology,–soils with particular vulnerability, and above all, its climatic variability amplify the exposition to various type of hazards. Among the Mediterranean, Tunisia is considered the most country exposed to climate change. The main natural hazards that would be face are the increase in the temperature, in the sea level, in extreme phenomena and the decrease in precipitation.

The impact of natural disaster on human, economies and livelihoods has witnessed drastic increase globally due to ongoing climate change phenomenon. The frequency and the magnitude of these natural disasters have also seen a significant rise in the recent past. Floods and forest fires are the major natural hazards that affect human lives and infrastructure.

Globally, disaster management has shifted from a reactive approach to a more pro-active one focusing on hazard assessment and risk mitigation, in order to minimize the impact of the natural disasters on economies and livelihoods. Space provide more information, which plays pivotal role in disaster management due to synoptic coverage and mapping of otherwise inaccessible areas along with timeliness. Sendai framework on disaster risk reduction 2015-2030 also advocates the use of space based datasets/technologies.

UNSPIDER program in collaboration with the international charter “space and major disasters” provided space based support by giving raw or processed data depending on satellite images availability. Likewise, this program support countries in capacity building of disaster mitigation managers using space based information in different phases of disaster from preparedness, rescue/relief and impact assessments to rehabilitation and migrations. Dissemination of space based information in near real time help in local authorities, volunteer organizations and improved decision-making in disaster management rescue, relief operations during major disasters. In addition, spatial information on disaster event helps in location assessment for establishment of relief camps/temporary shelters in most affected areas.

Tunisia’s experience can be summarized in the activation of UNSPIDER program by the National center of Mapping and Remote Sensing following the floods that hit Nabeul region in 2018, **and the** activation of the international charter by the National Office of Civil Protection following the forest fires happens last years. The Tunisian authorities received multispectral images and thematic maps produced by Copernicus mapping services.

# **Flood mapping using HECRAS 2D and Radar Sentinel 1: case study of the Medjerda river, Jendouba-Bousalem section.**

Aouissi Jalel<sup>1</sup>, Safa Zakraoui<sup>1</sup>, Zeineb Kassouk<sup>1</sup>, Hachem Agili<sup>2</sup>, Karem Chokmani<sup>2</sup>, Faiez Msallem<sup>3</sup>, Zohra Lili Chabaane<sup>1</sup>

**1** LR17AGR01 Integrated Management of Natural Resources: Remote Sensing, Spatial Analysis and Modeling (GREEN-TEAM), National Agronomic Institute of Tunisia (INAT), University of Carthage, 43, Avenue Charles Nicolle, Tunis 1082, Tunisia

**2** INRS-Institut National de la Recherche Scientifique (INRS), Québec, QC G1K 9A9, Canada

**3** Direction Générale des Barrages et des Grands Travaux Hydrauliques, Tunisia

## **Abstract.**

Flood risk is one of the major natural hazards worldwide. The monitoring and observation of the flood hazards are poor or not implemented in the vulnerability area to flood risk. In the north western of Tunisia, specifically the Medjerda river and its tributaries, flood risk is considered a problem that is worsening with climate change. The Jendouba Bousalam section is the most affected area by flood risk. The objective of this study is the flood mapping of the February 2015 event using HECRAS 2D modelling and Sentinel 1 in the Jendouba Bousalem section. Firstly, we assess the sensitivity of HECRAS 2D to the Digital Elevation Model (DEM) resolution using a 30 m DEM and LIDAR data (1 m resolution) and roughness coefficients on the water depth and flood extent. The flood hydrographs of the February 2015 event were obtained from the national directorate of water resources of Tunisia. They used as a boundary condition, in HECRAS 2d model. In addition, the Sentinel 1 SAR was used to generate reliable inundation maps. Results show that the HECRAS 2D model was mostly sensitive to DEM resolution for flood extent mapping. The statistical index F1 and F2 were used to analysis the performance of HECRAS model for simulating flood mapping using the two DEM according to the flood map estimated after processing the Sentinel 1. The F1 and F2 values are 0.8 and 0.64 respectively for flood extent modelling using LIDAR DATA. The simulation of flood mapping using the DEM 30 m, the F1 and F2 values are 0.53 and 0.12 respectively. Our results indicated that usage of LIDAR data produce more accurate flood inundation maps. This work constitutes a support for decision-makers for flood risk management and mitigation.

**Key words:** LIDAR, HECRAS 2D, DEM 30m, Sentinel 1, Flood mapping,

## Soil Erosion assessing through the Synergy of Google Earth Engine and Integrated RUSLE Modelling

Anis GHATTASSI<sup>1\*</sup>, Ahmed EZZINE<sup>2</sup>, Salwa SAIDI<sup>3</sup>

<sup>1</sup>Faculty of Sciences of Tunis; <sup>2</sup>National Center for Mapping and Remote Sensing; <sup>3</sup>Faculty of Sciences of Tunis

[anisghattassi7@gmail.com](mailto:anisghattassi7@gmail.com), [anisghattassi7@gmail.com](mailto:anisghattassi7@gmail.com)

**Keywords:** Soil erosion, Google Earth Engine, RUSLE model, Soil loss, Sustainable land management

Soil erosion poses a critical environmental challenge with far-reaching implications for agriculture, water quality, and ecosystem sustainability. Accurate monitoring of soil loss is crucial for effective land management and better land conservation planning. In recent times, remote sensing and advanced geospatial technologies such as Machine Learning, have significantly improved our ability to monitor and assess large-scale soil erosion and to properly estimate soil degradation.

This study presents an innovative approach integrating RUSLE (Revised Universal Soil Loss Equation) modeling with the performance of Google Earth Engine (GEE) matrix calculation in estimating soil loss in Mornag City.

The integration of RUSLE, a well-established empirical model, with GEE, a cloud-based geospatial analysis platform, offers an efficient means of processing extensive remotely sensed data and gaining valuable insights into soil erosion patterns across vast areas. Leveraging GEE's capabilities, which allow seamless integration of diverse geospatial datasets such as high-resolution satellite imagery, digital elevation models, soil information, and climate data.

This study presents a tailored workflow that combines the RUSLE equations with GEE's geoprocessing capabilities, enabling the rapid calculation of soil loss rates at a fine spatial resolution. The workflow incorporates key factors associated with soil erosion, including rainfall erosivity, soil erodibility, slope length, cover management, and conservation practices, which are dynamically derived from the integrated datasets.

To validate the effectiveness of our approach, we applied it to a study area encompassing various land cover types and topographic conditions. We compared the estimated soil loss rates with field measurements and existing soil erosion models, demonstrating the reliability and spatial accuracy of our integrated RUSLE-GEE approach. Our method effectively captures the heterogeneity of erosion patterns across the landscape.

Moreover, the scalability and accessibility of GEE enable the extension of our approach to larger regions, facilitating comprehensive soil erosion assessments and supporting evidence-based decision-making for sustainable land management. The real-time monitoring capabilities of GEE also hold promise for near-real-time soil erosion mapping, allowing for timely interventions and adaptive management strategies.

Considering all this, this study underscores the significant potential of integrating the RUSLE modelling approach with Google Earth Engine for accurate and scalable estimation of soil loss. By combining established empirical models with advanced geospatial technologies, we open up new avenues for understanding and mitigating the adverse impacts of soil erosion, contributing to the conservation and sustainable our soil resources.

## **Cooperation in remote sensing through student internship between Rhine-Meuse Water Agency and francophone universities to map irrigated and non-irrigated plots and estimate water abstraction by type of soils in Alsace**

François BAUDRY \*<sup>1</sup> Koffi Soeké ATTIGNON<sup>2</sup>, Ahlem ZINE LABIDINE<sup>3</sup>, Zeineb MEKKI<sup>4</sup>, François BIGORRE<sup>1</sup>, Loubna EL MANSOURI<sup>2</sup>, Zohra LILI CHABAANE<sup>4</sup>; Valerie DEMAREZ<sup>5</sup>,

<sup>1</sup> Agence de l'Eau Rhin-Meuse (AERM) à Metz; <sup>2</sup> Centre Régional Africain des Sciences et Technologies de l'Espace en Langue Française (CRASTE-L) à Rabat; <sup>3</sup> Université Aix Marseille, <sup>4</sup> Institut National d'Agronomie de Tunis (INAT), <sup>5</sup> Université Toulouse III CESBIO  
[f.baudry16@proton.me](mailto:f.baudry16@proton.me)

**Keywords:** satellite, irrigation, water abstraction, ecosystems

**Abstract:** The Water Framework Directive defined the notions of 'Water Body and 'Quantitative Good Status of Groundwater Body'(GWB) which is achieved when the water abstraction does not exceed the recharge of the GWB feeding associated ecosystems. For estimating the abstraction pressure on GWB the Rhine Meuse Water Agency (RMWA) has been relying on abstraction fees data. Other reliable methods for evaluating irrigation quantitative pressure on GWB were looked for.

Remote sensing has been developing in the francophone countries but there was little operational use in RMWA. In order to assess whether maize water needs and related water abstraction at regional level could be estimated by using satellite images, RMWA decided to get support from universities offering remote sensing cursus. It proposed in 2020, 2021 and 2022 Master II end of study internships. Following announcements on GeoRezo portal, each of these years, one candidate from a different francophone university was selected. As a result, researchers from Moroccan, French and Tunisian Universities supported scientifically the work of the student in internship in the RMWA (see above).

The maize cultivation and its high yield through irrigation represent a major economic asset in Alsace. Severe drought of these last years, more frequent due to climate change, led to the increased impact of irrigation on GWB and ecosystems. This impact has been more and more scientifically documented. Therefore, this situation created a tense context between irrigators and the institutional bodies in charge of GWB and ecosystems protection. In this context, remote sensing technics implementation was considered as an opportunity to improve scientific knowledge which could a common ground. This was a way to promote dialog between parties for future evolution of practices (cultivate less water consuming crops) in view of achieving GWBs quantitative good status.

In 2020, the first student used Sentinel 2 satellite images and produced, over part of the Alsace plain for several irrigated periods, maps of maize irrigated and non-irrigated plots. He also developed a method for the estimation of maize crops water needs considering the distinct types of soil. However, when the maps were presented to farmers, they remarked that in areas with high water storage capacity in soil, there were errors. Non irrigated plots were wrongly classified as irrigated. Thus, field survey was regarded as necessary for verification. Mapping the estimation of irrigation water needs using additional remote sensing data and technics was interesting to explore. In 2021, the study zone was extended to the whole Alsace. The student produced a map of irrigated and non-irrigated plots for 2019 and data for field survey were used for verification. Three farmers, having irrigated and non-irrigated plots in their farmland, provided the field data. Visits in their farms were effectively an opportunity to have a better understanding of remote sensing opportunities and facilitate future cooperation between partners. The student also developed a remote sensing method to produce maps of maize water needs for each area having a relatively homogenous type of soil. She used satellite images data to estimate P, ET and ETP. The values were aggregated by month. For the third internship, the time step was reduced to one week for the aggregation of parameters P, ET and ETP, which were estimated with satellite images. For each parameter maps were produced for the intense irrigation period. First results showed that the difference between the estimated value for the water abstraction by using satellite images and the one by using data of the water abstraction fees was found around 7 percent which is encouraging.

## **Monitoring of illegal drilling area in oases region in the south of Tunisia**

Zeineb Kassouk<sup>1</sup>, Ferdaws Akasha<sup>1</sup>, Wafa Chebbi<sup>1</sup>, Hammadi Habaieb<sup>1</sup>, Atfa Saad Agrebi<sup>2</sup>,  
Zohra Lili Chabaane<sup>1</sup>

1. University of Carthage, National Agronomic Institute of Tunisia, LR GREEN-TEAM. 43 Avenue Charles Nicolle, Tunis 1082, Tunisia.
2. Deutsche Gesellschaft für Internationale Zusammenarbeit (GIZ) GmbH ; 8, Rue des Lilas 1002 Tunis-Belvédère Tunisie

**Key words:** Illegal drilling, irrigated area, oases, Sentinel 1 & 2 synergy, Object oriented approach

With climate change and the scarcity of surface water and although the irrigation is regulated by strict rules, Tunisia is witnessing rapid expansion of illegal drilling. Remote sensing-based tools help effectively control illegal water uses.

The objective of this work is to use the synergy of optical (Sentinel-2) and radar (Sentinel-1) data at high spatial and temporal resolutions in the identification and quantification of oases irrigated by illicit drilling on groundwater and deep aquifers in the governorate of Kébili.

We used 3 Sentinel-2 images and one Sentinel-1 image, acquired during the month of March 2022 and 40 field observations to classify oasis areas using supervised pixel-oriented and object-oriented classification approaches.

In the first approach we used a pixel-based decision tree classification with the Normalized Vegetation Index (NDVI) calculated for the three Sentinel-2 data. Obtained result was compared to the soil moisture map derived from Sentinel-1 image. This method allowed the identification of illicit irrigation zones with a precision of 80% .

In the second approach an object oriented classification method was carried out using the three NDVI, principal component analysis (PCA) data (PCA1, 2 and 4), calculated from each Optical data, and the soil moisture map calculated from Sentinel-1. The result retained following this approach was validated by the superimposition with the data of illicit drillings, more than 90% of these zones contain illicit drillings. Illicit extensions represent five times the area of the legal Public Irrigated Perimeters (PPI).

Spatial maps of illegal oases have been generated to assess irrigation. The findings of this study might be useful for policy makers as well as planners.

## Spatial prediction of soil organic carbon contents at the scale of the plain of Sminja (NE of Tunisia) by fusing Sentinel-2 multispectral and laboratory hyper-spectral data

Tebibi Housseem Eddine<sup>1</sup>, Aichi Hamouda<sup>2\*</sup>, Youssef Fouad<sup>3</sup>, Didier Michot<sup>3</sup>, Emmanuel Vaudour<sup>4</sup>, Emna Karray<sup>5</sup>, Rafla Attia<sup>6</sup>, Hosni Trabelsi<sup>5</sup>, Thouraya Sahli Chahed<sup>5</sup>

<sup>1</sup>National Agronomic Institute of Tunisia; <sup>2</sup> Higher School of Agriculture of Mograne; <sup>3</sup>UMR 1069 INRAE, Institut Agro, Sol, Agro et hydrosystème, Spatialisation, <sup>4</sup>UMR INRA/AgroParisTech ECOSYS Equipe sol, <sup>5</sup>Centre National de la Cartographie et de la télédétection [houssemeddine.tebibi@inat.ucar.tn](mailto:houssemeddine.tebibi@inat.ucar.tn), [hammouda.aichi@esamg.u-carthage.tn](mailto:hammouda.aichi@esamg.u-carthage.tn), [youssef.fouad@agrocampus-ouest.fr](mailto:youssef.fouad@agrocampus-ouest.fr), [didier.michot@agrocampus-ouest.fr](mailto:didier.michot@agrocampus-ouest.fr), [Emmanuelle.Vaudour@agroparistech.fr](mailto:Emmanuelle.Vaudour@agroparistech.fr), [emnakarray2@gmail.com](mailto:emnakarray2@gmail.com), [attiarafra@yahoo.fr](mailto:attiarafra@yahoo.fr), [hosnitrabelsi@gmail.com](mailto:hosnitrabelsi@gmail.com), [t\\_sahli@yahoo.fr](mailto:t_sahli@yahoo.fr)

**Keywords:** Soil Organic Carbon, Sentinel 2, Data fusion, PLS, RF, SVR, ANN MLP, Machine learning, Deep learning.

Soil organic carbon is a key parameter to assess soil health. In semi arid context we explored the use of Sentinel-2 satellite imagery and lab Vis-NIR soil-spectrometric database to predict soil organic carbon (SOC) content in agricultural land in the Sminja watershed (Zaghouan Governorate, NE Tunisia). We investigated four modelling approaches: Partial Least Square Regression (PLSR), Random Forest (RF) and Support Vector Machine (SVM), as well as a Multi-layer Perceptron (ANN MLP) deep learning model based on an Artificial Neural Network (ANN). We have used different combinations of predictors variables, including laboratory hyper-spectral data, Sentinel-2 bands, spectral indexes, and soil physico-chemical parameters such as soil textural fractions. Our results show, that the ANN approach performs at least twice as well as the Support Vector regression, with a test  $R^2$  equal to 84% and an RMSE equal to 1.05 g.kg<sup>-1</sup>. The RPD equals 2.86 for training and 7.69 for validation. In addition, the RPIQ was equal to 6.02 indicating the good performance of the model. For the ANN model, the best results correspond to the combination of bands from lab spectra, spectral indexes, and physicochemical parameters. The SVM and RF models gave less satisfactory test results with  $R^2$  equal to -0.02 and -0.15 for RF and SVM, respectively. The accuracy of prediction models would increase with the inclusion of more environmental predictor data, which would have a favorable effect on the region's decision-making regarding agricultural practices.

## Assessment of the effect of salinity on soil organic carbon prediction, using Sentinel-2 derived data

Sahar Bounaaja<sup>1</sup>, Aichi Hamouda<sup>2\*</sup>, Didier Michot<sup>3</sup>, Youssef Fouad<sup>3</sup>, Emmanuel Vaudour<sup>4</sup>, Emna Karray<sup>5</sup>, Rafla Attia<sup>6</sup>, Thouraya Chahed<sup>5</sup>, Hosni Trabelsi<sup>5</sup>

<sup>1</sup>National Agronomic Institute of Tunisia; <sup>2</sup>Higher School of Agriculture of Mograne; <sup>3</sup>UMR 1069 INRAE, Institut Agro, Sol, Agro et hydrosystème, Spatialisation, <sup>4</sup>UMR INRA/AgroParisTech ECOSYS Equipe sol, <sup>5</sup>Centre National de la Cartographie et de la télédétection, <sup>6</sup>DG ACTA Direction des sols, Tunisie.

[saharbounaaja@gmail.com](mailto:saharbounaaja@gmail.com), [hammouda.aichi@esamg.u-carthage.tn](mailto:hammouda.aichi@esamg.u-carthage.tn), [youssef.fouad@agrocampus-ouest.fr](mailto:youssef.fouad@agrocampus-ouest.fr), [didier.michot@agrocampus-ouest.fr](mailto:didier.michot@agrocampus-ouest.fr), [Emmanuelle.Vaudour@agroparistech.fr](mailto:Emmanuelle.Vaudour@agroparistech.fr), [emnakarray2@gmail.com](mailto:emnakarray2@gmail.com), [attiarafra@yahoo.fr](mailto:attiarafra@yahoo.fr), [t\\_sahli@yahoo.fr](mailto:t_sahli@yahoo.fr), [hosnitabelsi@gmail.com](mailto:hosnitabelsi@gmail.com), .

**Keywords:** Soil organic carbon, Salinity, PLS, RF, Ordinary kriging, Sentinel-2

Soil salinization is closely related to land degradation, and it is supposed to exert a significant effect on soil organic carbon (SOC) stock dynamics. In semi-arid regions, this effect and its variability have been rarely quantified neither at site nor over large spatial extents. The main focus of this study is evaluating the impact of the salinity on SOC prediction models in the plain of Sminja (480 km<sup>2</sup>), located in the north-east of Tunisia. We employed the Sentinel-2 derived data, combined with 11 analytical covariates within the field campaign measurements collected in the study area.

We constructed different regression models capable of assessing the salinity-induced SOC prediction changes in the Sminja plain. Thus, in order to characterize the SOC spatial distribution, we calibrated partial least squares regression models using 11 analytical covariates, 11 Sentinel-2 derived spectral indexes with the 4 bands b2, b3, b4 and b8. In the purpose of mapping the salinity spatial variability in Sminja, we used the ordinary kriging methods, the random Forest (RF) and the Partial least squares (PLS) algorithms. In fact, 5 spectral salinity indices (NDSI, SI1, SI2, SI3 and SI11), 11 auxiliary variables combined with the spectral reflectance of the bands b2, b3, b4 and b8 of Sentinel-2 were included as predictive variables in the models. As a way to evaluate the salinity effect on the SOC prediction performances, models were calibrated applying three classes of salinity (C1(0-1,2 dS.m-1), C2(1-2dS.m-1), C3(>2 dS.m-1)).

Results showed that the PLS models performed well in predicting SOC content, with the R<sup>2</sup> value reaching 88%. The kriging method possessed an excellent capacity of estimating soil salinity variations comparing with the machine learning and the linear estimation approaches (R<sup>2</sup> only reached 48%). The SOC map showed that the SOC ranges were highly advanced especially in the South-west of the plain (reaches 40 g.kg-1). The salinity map obtained on account of the kriging method showed that salinity follows an increasing gradient from the North-east to the south-west of Sminja so that we distinguish 5 soil categories (USSL classification): non saline soils (0-2dS.m-1) allocated in the major part of the plain, slightly saline soils (2- 4dS.m-1), moderately saline (4-8dS.m-1), strongly saline (8-16dS.m-1) and extremely saline soils (>16dS.m-1) were assigned in the North-east of Sminja. Apart from this, the results recorded that the application of the PLS model with C1 and C2 showed high performances in predicting SOC content (R<sup>2</sup> reaches 0,91 in C1 and 0,88 in C2 and RMSE varies between 1,07 and 2,87 g.kg-1), while in the C3, the PLS model provided weaker prediction accuracies (R<sup>2</sup>-calibration = 0,85, R<sup>2</sup> -validation = 47% and RMSE hits the value 8,39 g.kg-1).

Our results suggest that the role of soil salinization should not be neglected in SOC changes projection, and soil salinization control measures should be further taken into practice to enhance soil carbon prediction over large extents.

## **Contribution of remote sensing and modelling techniques in water erosion cartography: case of upper-valley of Medjerda-Tunisia**

Dhouha Ben Othman<sup>1\*</sup>, Ahmed Ezzine<sup>1</sup>, Emna Kochlef<sup>1</sup> and Aymen Lassoued<sup>1</sup>

<sup>1</sup> *National Center of Cartography and Remote Sensing- Tunisia (CNCT-Tunisie),*  
[cnct@defense.tn](mailto:cnct@defense.tn), [benothmand@gmail.com](mailto:benothmand@gmail.com)

**Keywords:** Water erosion, Modelling, GIS, Remote sensing, Upper valley Medjerda, Tunisia.

### **Abstract.**

Water erosion is considered as the most significant environmental problems and main origin of soil degradation throughout the Mediterranean region. It may have serious consequences affecting countries sustainable development, water resources mobilization and agricultural production. The present study aims to monitor water erosion dynamic in the upper valley of Medjerda watershed. The adopted methodology was based on modelling, GIS and remote sensing techniques using a multicriteria decision-making approach combined between satellite data, meteorological, geological, pedological and land use data. Key results of this contribution made it possible to develop a map of spatial erosion dynamic regionalization describing soil vulnerability. This map shows that 62% of Medjerda upper valley present moderate to very high soil erodibility. Indeed, highly vulnerable zones are characterized with fragile soil, steep slopes and undergoing very extensive agricultural activity where land cover is not protective.

In the second part, sensitivity to water erosion was confirmed by identification of areas affected by flood risk. This later was accomplished by satellite image processing techniques to calculate some water indices. Finally, findings of this study represent a decision support document for developing of soil and water resources management strategies in the study area.

\* This work is part of the CNCT (2023-2024) research contract program (Erosion Project: 2019-2023), funded by the Ministry of Higher Education and Scientific Research

## Mapping of Mineral Resources by Remote Sensing: A Geospatial Approach

Nouha BEN YAHIA<sup>1</sup>, Wafa TALHAOUI<sup>1</sup>

<sup>1</sup>*National Center for Cartography and Remote Sensing*

[nouha.benyahia@fst.utm.tn](mailto:nouha.benyahia@fst.utm.tn)

**Keywords:** Remote sensing, mineral resources, mapping, satellite imagery, geological exploration.

Mapping mineral resources using remote sensing techniques has emerged as a crucial tool in modern geospatial science, mineral exploration, and resource management. This abstract provides a concise overview of the key aspects and advancements in the field of mineral resource mapping using remote sensing technologies. This work takes place within the current project, entitled “Mapping and valorization of mineral resources by remote sensing”, led by the National Center for Cartography and Remote Sensing.

The paper discusses the advantages of remote sensing, including its non-invasive nature, wide-area coverage, and cost-effectiveness compared to traditional geological surveys. It highlights case studies and examples from different regions and mineral types, showcasing the diversity of applications ranging from the identification of ore deposits to environmental monitoring associated with mining activities.

Furthermore, this review explores the challenges and limitations of remote sensing in mineral resource mapping, such as atmospheric interference, sensor limitations, and the need for ground truth validation. It emphasizes the importance of integrating remote sensing data with geological and geophysical data to create comprehensive mineral resource maps.

In conclusion, remote sensing's ability to identify and map mineral resources based on their spectral characteristics offers a powerful and non-destructive approach to geospatial analysis. It enhances our capacity to understand, conserve, and responsibly exploit Earth's mineral wealth, contributing to both scientific knowledge and sustainable development goals.

## Earth Observation for territorial monitoring and management dealing with SDG : CNCT role

Thouraya Sahli Chahed<sup>1\*</sup>, Wafa Talhaoui

*Centre National de la Cartographie et de la Télédétection Tunisia*

[t\\_sahli@yahoo.fr](mailto:t_sahli@yahoo.fr), [cnct@defense.tn](mailto:cnct@defense.tn)

**Keywords:** Earth Observation, Remote Sensing, Sustainable Development Goals

The CNT was created in 1988, and in 2004 happened a fusion between the Geography and Hydrography services of the Army, which resulted in a new organization of the CNT. In 2009, the CNT saw its missions expanded by adding the mission of cartography (CNT became CNCT). Certified ISO 9001 since 2008 and renewed three times CNCT migrate to the 2015 version with the fifth renewal on December 2019.

As a national institution in charge of the large field of geomatic, the CNCT works to organize the geographic information's sector at national level. while to be a valued partner the center set up its vision which aims "To make the National Center of Mapping and Remote Sensing a **leader institution** that owns and **uses the latest geospatial technologies** and contributes to the dissemination of the **research culture** in the field of geomatics and its smart products, **focused on innovation and continuous improvement** of their performance for a **better future**".

In this sense, it is very useful to insure the accessibility to the citizens, customers, students, researchers and to cooperate with privileged national and international partners and bilateral coop. That is why, the CNCT focus on capacity building of its technical staff and to elaborate partnership with universities through multi thematic projects.

through it's 11 missions set by decree, the CNCT make diversity of maps covering different sectors related to terrain, marine, and thematic maps and the city plans, aerial photography plane as the co-owner with Topographic and Cadastral office.

In order to accomplish its mission of organizing the geomatic sector, the CNCT works to set up the necessary environment for the development of various socio-economic sectors based on the use and exploitation of geographic information. This environment concern the establishment of a national infrastructure for geographical information, which characteristics are, developed according to the needs of potential national public and private users.

In other area, the mission of promoting the use of space-based data has remained relevant since the creation of the CNCT and works towards the establishment and implementation of projects alignment with UN SDG. The management, monitoring and exploitation of the territory (urban, environmental issues etc.) as well as natural resources (forest, water, soil, agriculture etc.) and phenomena (desasters, desertification etc.) are the themes of interest involving the exploitation of spatial data using remote sensing technics and set up platforms and modes to ensure their improvement.

## **ACCWA: An innovative set of remote sensing based monitoring tools for agriculture and water management in the Mediterranean region. Ebre Basin Case Study.**

*Maria José Escorihuela<sup>1</sup>, Guillem Sánchez<sup>2</sup>, Víctor Altés Gaspar<sup>3</sup>, Giovanni Paolini<sup>1</sup>, Manel Khlif<sup>1</sup>, Olivier Merlin<sup>3</sup> and Zohra Lili-Chabaane<sup>3</sup>*

<sup>1</sup>*isardSAT, Parc Tecnològic Barcelona Activa, Carrer de Marie Curie, 8, 08042 Barcelona, Spain*

<sup>2</sup>*Institut National Agronomique de Tunisie (INAT) Université de Carthage.*

<sup>3</sup>*Centre d'Etudes Spatiales de la Biosphère (CESBIO), France*

The Mediterranean is among the most sensitive areas to climate change as demonstrated in many studies (IPCC, 2013). The models issued by IPCC cast different scenarios for the Mediterranean Region, but all of them agree on a clear increasing trend of temperatures. Precipitation projections are uncertain due to high inter-annual variation, but inter-annual and spatial variability are expected to increase. It is expected the duration of the rainy season be shorter and summer dry spells be longer, increasing agriculture land deterioration and desertification.

Increased rainfall variability and ET rates will compromise irrigation potential and expansion plans and increase competition and conflict over limited water resources. There are significant knowledge gaps and uncertainties about how much water will be available for a complete growing season, how much should be used for scheduling irrigation efficiently and extracted from these regions. More information regarding water use is necessary to improve agricultural planning and to manage water more efficiently at different scales: farm and catchment/irrigation district level.

The expected impact in rainfed agriculture is a decrease in yield due to heat and water stress and an increase in the likelihood of crop failure in rainfed crops for maize, millet and sorghum. Ongoing changes in the socio-economic and environmental background of rainfed farmers combined with the expected population growth make timely and reliable information on rainfed crop yield and its spatial variability essential in decision-support for improving food security and livelihoods.

At the same time, temperature and precipitation changing patterns will increase hazards linked to environmental conditions such as droughts, floods or crop pests like. In order to reduce the impact of these hazards a critical component is a comprehensive hazards monitoring system that can provide early warning and deliver that information to users in a timely manner.

In this climate change context, ACCWA aims to develop the remote sensing based monitoring tools for agriculture and water management that help risk guidance.

ACCWA aims to develop the remote sensing based management and monitoring tools for food security and water & agricultural risk management that allow improving the reliability of decision making regarding water use, yield and hazards in agriculture. The water and agriculture management system is being defined in accordance with user needs and requirements.

In this presentation we will show the development of a soil moisture anomaly product and drought index derived from high-spatial remote sensing soil moisture over the entire Ebre Basin.

The ACCWA project has been awarded a H2020-MSCA-RISE-2018 grant (grant agreement No 823965)

# **Exploring the Global New Space Economy and Its Impact on the African Space Sector**

**Abstract:** This presentation delves into the transformative landscape of the global new space economy and its direct influence on the African space sector. Participants will gain a comprehensive understanding of the key elements driving the new space economy worldwide, including emerging technologies, market trends, and investment landscapes. The presentation specifically focuses on applying these global trends to the African space industry, highlighting the unique opportunities and challenges within the African context. By examining case studies and success stories, participants will witness the tangible impact of the new space economy in Africa. The presentation aims to inspire participants to leverage global best practices, foster collaboration, and contribute to the growth and development of the African space sector within the broader global new space economy.

## **Potential Presentation Outline:**

### **I. Introduction**

- A. Overview of the new space economy and its global significance.
- B. The growing importance of the African space sector in the context of the new space economy.

### **II. Key Elements of the New Space Economy**

- A. Exploration of emerging technologies driving the new space economy
- B. Analysis of market trends and investment landscapes shaping the global space sector.
- C. Identification of key players and their influence on the new space economy.

### **III. The African Space Sector: Opportunities and Challenges**

- A. Overview of the African space sector's current status and growth potential.
- B. Identification of unique opportunities and challenges specific to the African context.
- C. Highlighting successful initiatives and projects in the African space sector.

#### **IV. Applying Global Trends to the African Space Sector**

- A. Strategies for incorporating global best practices in the African space industry.
- B. Leveraging partnerships and collaborations to enhance the African space sector.
- C. Exploring avenues for technology transfer and knowledge exchange.

#### **V. Fostering Growth and Collaboration in the African Space Sector**

- A. Promoting innovation, entrepreneurship, and capacity building in the African space industry.
- B. Encouraging policy development and regulatory frameworks to support the growth of the African space sector.
- C. Building networks and partnerships to foster collaboration within Africa and internationally.

#### **VI. Conclusion and Call to Action**

- A. Recap of key insights and takeaways from the presentation.
- B. Encouraging participants to seize the opportunities presented by the new space economy.
- C. Inspiring participants to contribute to the growth and development of the African space sector through collaboration, innovation, and strategic partnerships.

**Note:** The presentation outline provided above serves as a general framework for the presentation on navigating the new space economy and its implications for the African space sector. However, please note that the specific elements and depth of coverage within the outlined topics may be adjusted based on the allocated time for the presentation. The presenter will make necessary modifications to ensure a concise and impactful delivery while addressing the most relevant and important aspects within the given time constraints.

#### **Presenter: Malak Trabelsi Loeb**

**Bio:** Malak Trabelsi Loeb is a Dubai-based visionary entrepreneur and accomplished legal consultant. With expertise in International Business, Space, Tech Law, and National Security, she brings 17 years of international business experience and 12 years of legal expertise. Mrs. Loeb is the Founder and Managing Director of Vernewell Management Consultancies, an International Space and Deep Tech-focused Management, Innovation, and Artificial Intelligence Research and Consultancies Firm; the CEO of Trabelsi Loeb Legal Consultancies; and the founder of Vernewell Academy, the newly launched Learning Center. Mrs. Loeb is recognized as an international thought leader and sought-after speaker. She has delivered workshops and lectures as a space subject matter expert for prestigious organizations, including the NATO Strategic Direction-South Hub/ NATO Joint Allied Transformation command, Italy; and the Royal Aeronautical Society –

UAE Branch. She delivered keynotes at various law, space, technology, and business-related conferences, including The Future Innovation Summit Dubai; Abu Dhabi Air Expo 2022 Conference; Global Blockchain Convention Dubai, International Space Convention, Turkey; Business Immersion Week EU Business School, Switzerland; Inside Quantum Technology - New York, Airport Show - Women in Aviation Conference, Dubai.

Photo:



## Big Data and Artificial Intelligence Technologies for Drone-Based Applications

Yassine Gacha<sup>1</sup>, Takoua Abdellatif<sup>1,2\*</sup>,

<sup>1</sup>*SERCOM Laboratory, University of Carthage, Carthage 1054, Tunisia;* <sup>2</sup>*ENISo, University of Sousse, Sousse 4002, Tunisia*  
[Takoua.Abdellatif@ept.rnu.tn](mailto:Takoua.Abdellatif@ept.rnu.tn)

**Keywords:** Big Data, Artificial Intelligence, Drone-based Applications.

In this research work, we explore the intersection of big data and artificial intelligence (AI) in the context of drone-based applications. Drones, equipped with sensors and cameras, generate vast and rapid amounts of data during their operations. Harnessing this data effectively and leveraging AI with big data technologies can unlock valuable insights and enhance the capabilities of drone applications across various sectors.

We will delve into the following key areas:

1. **Introduction to Drone-Based Applications:** We provide an overview of the diverse applications of drones in sectors such as agriculture, infrastructure inspection, environmental monitoring, search and rescue, and more. This will set the stage for understanding the potential impact of integrating big data and AI technologies.
2. **Big Data Challenges and Opportunities:** We explore the challenges associated with handling and processing the large volumes and high rate of data generated by drones. This will include discussions on data storage, data collection, real-time data processing, data quality, and data privacy. Additionally, we will highlight the opportunities that big data presents for drone-based applications, such as predictive analytics, anomaly detection, and actionable insights.
3. **AI Techniques for Drone Data Analysis:** We delve into various AI techniques that can be applied to analyze drone data effectively. This will encompass topics such as machine learning algorithms, computer vision, deep learning, and natural language processing. We will discuss how these techniques can enable intelligent decision-making, object recognition, image processing, and data fusion for drone-based applications.
4. **Use Case:** We present DroMOD<sup>1</sup>, a Tunisian drone-based surveillance system implemented in collaboration between the military aviation school of Borj Amri and the Polytechnic School of Tunisia. This case study will highlight the benefits, challenges, and outcomes achieved through the integration of these technologies. DroMOD assures efficient real-time multi-scope object detection by combining deep learning algorithms with stream big data technologies and intelligence drone-side data filtering. A demo will show DroMOD usage for Fire, person, and car real-time detection in the city of Bizerte in Tunisia.

By the end of the talk, participants will gain insights into the transformative potential of big data and AI technologies in the realm of drone-based applications. They will understand the challenges, opportunities, and future directions in leveraging these technologies to enhance efficiency, decision-making, and outcomes in various industries, mainly in Tunisia and Africa.

# Hardware-aware, deep-learning approaches for image denoising and star detection for star tracker sensor

Besma Guesmi, David Moloney  
Ubotica Technologies  
Dublin, Ireland  
[besma.guesmi@ubotica.com](mailto:besma.guesmi@ubotica.com)  
[david.moloney@ubotica.com](mailto:david.moloney@ubotica.com)

**Abstract**—In recent years, Deep Neural Networks (DNNs) approaches have outperformed traditional techniques for several computer vision problems. This has been made possible by the increase of computational resources represented by Graphical Processing Units (GPU) that allow training using large datasets and the availability of deep learning accelerators for inference. On the other hand, the attitude determination accuracy requirements for spacecraft are increasing. The most accurate attitude determination sensor for spacecraft is the so-called star sensor or star tracker. With the increase in low-cost satellite platforms such as CubeSats, research into the improvement of star sensor accuracy for low-power and low-cost sensor architectures remains a relevant subject. In this context, we examine several methods for noise reduction and star detection for improving centroiding performance. More specifically, an efficient and robust denoising method for star images using an Auto-Encoder (AE) is proposed. This method enhances the image quality for systems sensitive to noise. Furthermore, an accurate and lightweight algorithm based on an existing YOLO (You Only Look Once) architecture is proposed to detect the location of stars in the image. In this work, the YOLO bounding boxes are used to describe the space region around the stars. Subsequently, the star centroid within the bounding box is computed using the COG (Center Of Gravity) method. This method removes the need for centroiding algorithms sliding over the entire image area. An extensive comparison of the proposed denoising technique with other traditional filters confirms that the proposed method resists all noise models and reconstructs well the corrupted images. Experiments show that the proposed YOLO-based star detector achieves high accuracy with a lightweight architecture without any extra latency.

**Keywords**—Attitude determination, Centroiding, Deep learning, Denoising, detection, YOLO.

## I. INTRODUCTION

Accurate attitude determination is a critical topic for the success of space missions. Many attitude-determination sensors exist, such as the sun, magnetometers, gyroscopes, horizon, and inertial sensors [1]. However, the most accurate attitude determination sensor is the star sensor. In classical star sensors, attitude determination is based on the perceived location of stars on the celestial sphere. Thus, accurate

centroid determination is required to ensure an accurate determination of the location of stars as imaged by the star sensor [2]. However, images obtained by the imaging system often have a low signal-to-noise ratio due to various physical constraints. Different models of noise [3] (including dark noise, shot noise, salt and pepper noise, readout noise, etc.) appear during the image capture process due to the faint incoming light and the analog-digital data conversion. As image denoising is a basic technique, that has been studied extensively in the literature, many denoising methods have been proposed [4]. These methods include ([5]): Gaussian filtering, median filtering, Wiener filtering, etc. The thresholding method is often used for both noise removal and object detection [6][7] by setting a threshold to distinguish the stars (connected white pixels) from the background [8]. Many thresholding methods are used in star trackers such as adaptive thresholding [9], Otsu thresholding [10], and the moment-preserving method [11]. For example, Dikmen [12] proposed a combination of linear filters and thresholding methods for noise removal. Ting et al.[13] also proposed the correlation and convolution filters for image denoising. Furthermore, centroiding introduces additional errors when traditional filtering methods [14] are applied. Traditional filtering methods are designed to remove only one kind of noise (e.g., the median filter is the appropriate solution for removing "salt and pepper" noise) [12]. However, captured images are usually affected by various noises, so it would be difficult to denoise the image by applying only one type of filter. Furthermore, the use of non-linear filters [13] such as the median filter or histogram equalization could cause unexpected deviations in the centroid star position.

For star detection, most papers propose thresholding techniques to detect the stars within the image [4], however, this is not suitable for centroid calculation where the pixel intensity must be converted to 0 or 255, which leads to a loss of information and inaccurate centroid values because the COG centroid formula is related to the pixel values. Additionally, the computational cost of finding the connected pixels in an image is high. Applying different filtering techniques and thresholding methods to ensure accurate detection (including the detection of dim stars), is

time-consuming for edge devices and real-time testing. Thus, the typical star tracker pipeline uses thresholding for both filtering and detection as illustrated in Fig.1.



Fig.1: Traditional Star tracker flowchart

On the other hand, several deep learning algorithms have been developed to ensure high accuracy for object detection applications. RCNN [15], Fast-RCNN [16], and Faster-RCNN [17] are the most common object detection algorithms, used in many applications. These techniques use regions to localize the object within the image. However, for star trackers, the objects of interest (i.e. the stars) are distributed over the whole image. Thus, in a practical scenario, these algorithms cannot meet the real-time criteria of object detection. Therefore, a regression-based first-order algorithm such as SSD[18], YOLO[19], etc, is more appropriate for our purposes. These algorithms provide faster inference speeds and less complex architectures that meet the requirements of real-time embedded applications.

To compute the star centroid within the bounding box, the COG method is used by applying the denoising technique to increase the accuracy and achieve a trade-off between accuracy and low computation cost. Furthermore, The COG method is much faster than other centroiding algorithms in terms of computation time [20].

The purpose of this paper is to apply advanced neural network methods to solve some of the major problems of star tracker systems (e.g. noise, latency, accuracy) with low computational cost, and low memory overhead. A supervised Denoising Auto-Encoder (DAE) is applied for noise removal due to its ability to learn important features of images. A lightweight star detection architecture based on YOLOv5 is used for star detection. Then, the YOLO bounding boxes are extracted for centroiding. Our proposed star tracker pipeline is summarized in the flow diagram in Fig.2.

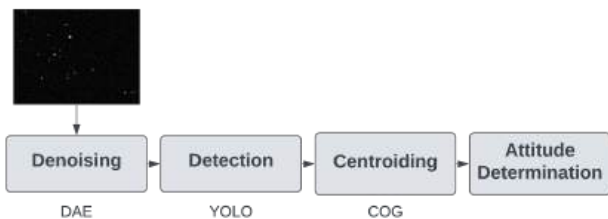


Fig.2: Proposed Star tracker flowchart

The paper is organized as follows. In Section II, the proposed star tracker pipeline is illustrated. Section III shows the star tracker algorithm results. Finally, concluding remarks and ideas for future work are drawn in Section IV.

## I. METHODOLOGY

### A. Denoising Auto-Encoder (DAE)

The DAE is an image denoising technique [21] Based on a Convolutional Neural Networks (CNN) architecture used to restore the original image, which in our case shall allow accurate centroiding. The proposed CNN architecture is based on the Auto-Encoder (AE) neural networks which are commonly used for feature extraction and selection [22]. The DAE block is illustrated in Fig.3.

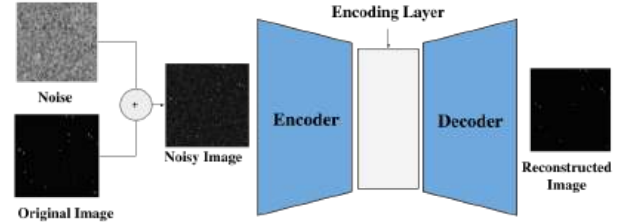


Fig.3: Illustration of DAE flow chart

The input image is sampled from the original (clean) dataset. Random noise (e.g., Gaussian noise, salt & pepper noise, shot, and dark noise) is added to the clean images to generate its noisy versions. The autoencoder is a feedforward network that is expected to reconstruct the clean versions of the noisy images. Formally, a DAE with encoder  $e(\cdot; \phi)$ , decoder,  $d(\cdot; \theta)$ , and corruption process,  $C(\cdot)$  is trained to minimize the cost function  $E_x l$ .

$$E_x l = (x, d(e(C(x); \phi); \theta)) \quad \text{Eq.(1)}$$

where  $x \in X$  are data samples whose underlying distribution is  $p(X)$ . Parameters  $\phi$  and  $\theta$  are learned. The optimal reconstruction function,  $R^*(\cdot)$  is learned by DAE trained to minimize the negative log-likelihood using a cost function. This optimization leads to minimizing the distance between the reconstructed images and the original images.

The model is trained using over 20,000 images corrupted by different noise models. The purpose of using both generated and real images is to improve the robustness and efficiency of the model.

Since the captured images are usually affected by noise, the DAE is trained with the generated dataset and then the trained model is used to denoise the collected star images, resulting in clean versions as shown in Fig.4.

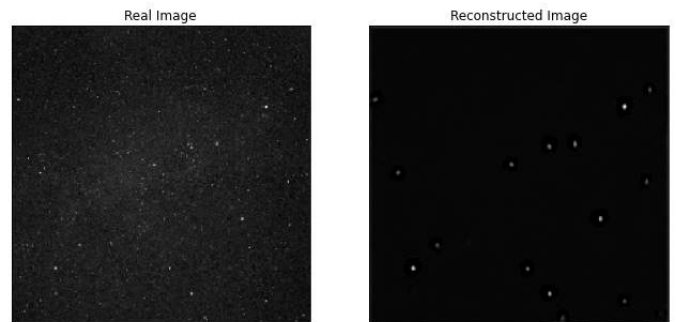


Fig.4: Collected image after denoising

To cover more than one type of noise and to test the validity of the proposed model under different noise conditions, four types of noise (Gaussian noise, salt & pepper noise, shot noise, and dark noise) are added to each 20% of the generated dataset, a type of noise with multi-parameters (e.g. Gaussian noise ( $\sigma = 10,30,80$ )) is added. Each image contains only one type of noise. For the last 20% of the dataset, all the noise models are added to each image to build a mixed dataset with different noise types and levels.

For the DAE model, a low-complexity architecture and a small network size are required. Dense layers are not powerful enough to learn important features of the images. Using a CNN network with fewer layers for the encoder and the decoder is the most suitable solution to build a robust denoising solution.

The full architecture of the DAE model is shown in Fig. 5. Generally, adding more convolution layers leads to more complex architecture and higher computational costs. Our results show that the desired performance is obtained by adding a few layers, representing a good trade-off between performance and computational load.

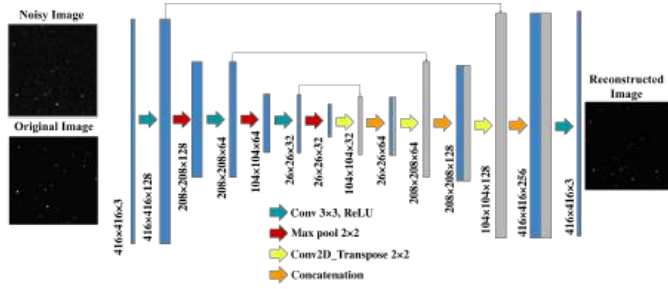


Fig.5: Encoder-Decoder Architecture

The model is composed of two main parts: an encoder and a decoder. The encoder is a CNN network with convolutional layers employing respectively 128, 64, 32, and 16 filter layers (values fixed experimentally), each of which applied a  $3 \times 3$  kernel, with padding used to keep image dimensions consistent between input and output. After each convolutional step, a rectified linear unit (ReLU) was added, followed by a  $2 \times 2$  max-pooling layer to down-sample the output by a factor of two. The decoder carries out the inverse operations of the Encoder. It uses a  $2 \times 2$  upsampling between convolutional operations, to reconstruct an input image with the same dimensions. The last convolution step consists of one layer only, which produces the reconstructed image (output).

The DAE training is divided into two stages. First, the model is trained using noisy images as input to learn how to reduce noise from images by comparing the reconstructed images with the original ones and reducing the loss function between them. Then, the trained model is used to remove the noise from the collected images (Fig.6). Finally, the model is retrained using the generated and collected dataset to build a robust and efficient denoising model. The same data split,

model architecture, and training parameters are used for both training stages. The input images are resized to  $416 \times 416$  pixels for both training stages.

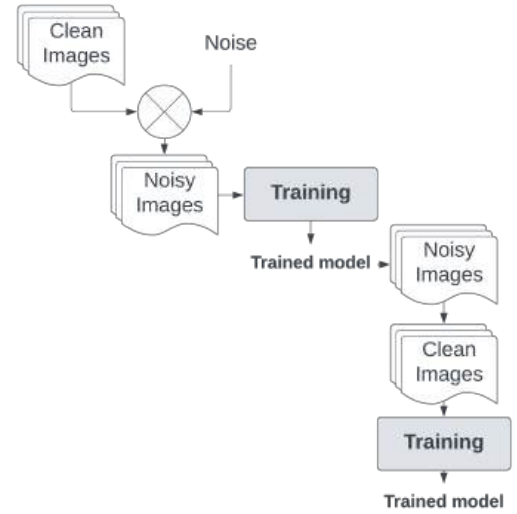


Fig.6: DAE training process

### B. Star detection

For Star detection, a YOLO model is used. The popular use approach was developed in 2015 by Joseph Redmon et al.: YOLO (You Only Look Once) [23]. The core idea of YOLO is to use the entire image as an input of the network, and directly return to the position of the bounding boxes and the class to which the object within the bounding boxes belongs.

One of the recent YOLO versions is YOLOv5, which is the extension and improved version of YOLOv3 and YOLOv4. The biggest novelty of YOLOv5 is translating the Darknet framework to the Pytorch framework which offers the ability to reduce the floating-point precision during the training inference process from 32-bit to 16-bit precision. This speeds up the inference of YOLOv5 compared to the previous versions. In addition, the anchor boxes in YOLOv5 are auto-learned with a custom dataset.

The fundamental idea of our approach is to extract as many stars as possible with a low-complexity architecture. Four models of YOLOv5 have been applied: nano, small, medium, and large architectures, where each of them offers different accuracy and performance. To ensure high accuracy and low computational cost, a new lightweight YOLOv5 architecture is proposed based on the existing architecture.

The whole object detection and centroiding pipeline based on YOLOv5 which includes dataset labeling, model training, and centroiding calculation is shown in Fig.7.

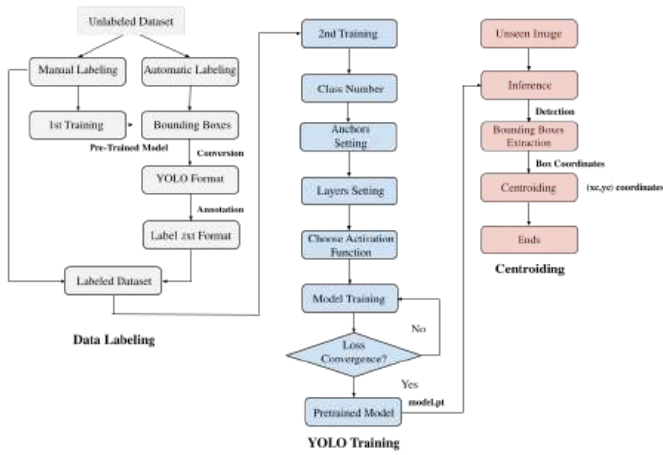


Fig.7: Data labeling, model training, and centroiding flow chart

For detection, a subset of the reconstructed DAE images were used for labeling. Since each image contains many stars, only 30% of the dataset is labeled manually, while the rest of the dataset is labeled automatically using the data labeling method (Fig.7). The proposed auto-labeling technique is based on the trained model with the subset that is labeled manually in order to detect the desired object in the images and draw the bounding boxes and save the outputs in YOLO format in text files to be considered as label files for each image. The labeled dataset has been used to train the model. Then, the pre-trained model was used to generate the corresponding labels of the unlabelled dataset (Fig.7).

The network architecture of YOLOv5 is shown in Fig.8. There are two reasons for choosing YOLOv5 as a baseline. Firstly, YOLOv5 uses CSPDarknet (Cross Stage Partial Darknet) as the backbone for pre-training by incorporating cross-CSPNet into Darknet. CSPNet can handle the problem of redundant gradient information that results in inefficient optimization and costly inference computations. Therefore, using CSPNet decreases the parameters and FLOPs (floating-point operations per second) of the model which not only improves the inference speed and accuracy but also reduces the model size for edge device implementation [24]. Secondly, YOLOv5 uses a Path Aggregation Network (PANet) as its neck to generate feature pyramids which helps the model identify the same objects with different sizes and scales. In addition, PANet improves the utilization of accurate localization signals in lower layers, which results in increased location accuracy.

The modified architecture continues to use the three main parts of the YOLOv5 updated version with fewer layers and parameters. The first block is the “Backbone” consisting of an input convolutional layer, four convolutional-pooling, and ending with a spatial pyramid pooling fast (SPPF) block. The SPPF is designed to improve the receptive field of the network by removing the fixed-size constraint of the network. The SPPF is used instead of SPP (Spatial Pyramid Pooling) [25], which mathematically provides the same results with fewer FLOPs and faster speeds.

The second block is the Neck which consists of two animated upsample-convolutional operations, which are mixed and

combined with image features. The Neck network is mainly used to generate FPN ( Feature Pyramid Networks), and then the output feature map is transmitted to the detected network. The third block is the detection part which applies anchor boxes on the feature maps output from the previous layer. The full proposed network is shown in Fig.8 with an input size of  $416 \times 416 \times 3$ .

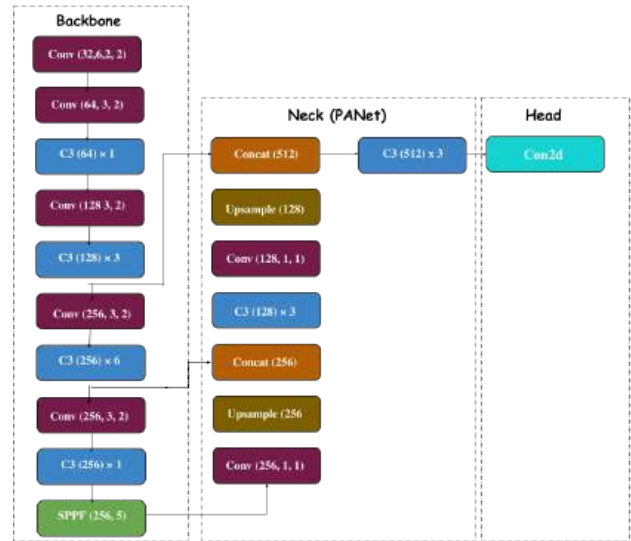


Fig.8: Overview of the modified version of the model YOLOv5n. It consists of three parts: (1) Backbone: C3, (2) Neck: PANet, and (3) Head: YOLO Layer

Firstly, the three convolution-pooling blocks decrease the map size to 132 the input image size and increase the number of feature maps to 512 by extracting and gathering the image features. After that, the SPPF block with three max-pooling layers is introduced as the last layer of the backbone, for concatenating the local region feature extracted and converged by multi-scale pooling. The  $1 \times 1$  convolution was adapted before the pooling to reduce the input of feature maps from 64 to 32 [26]. Then the feature maps are pooled by the sliding windows (5,5). The stride of pooling is all 1 and the padding is 2 which is used to keep a constant size of the output feature maps. After that, the three feature pooled maps are concatenated with the input feature maps of SPPF. Finally, another convolutional operation was added and applied to the concatenated layers to reduce the feature maps. The second block is the Neck network which is mainly used to improve the model’s detection with different sizes and scales. In the original architecture, three different sizes and scales are used for the same target to ensure the detection of large, medium, and small objects. Here, only small objects are of interest, so only a small scale is used for star detection. The two upsample-convolution blocks for medium and large objects were removed as shown in Fig.9. The C3 of a small object is concatenated with the output stage for detection. The last YOLOv5 version (v6.0) uses C3 which was introduced in the 4th version instead of the CSPBottleneck() layer which contains only three main convolution layers instead of four. The last block of the network is object detection which is composed of only one detected layer, whose input feature maps  $20 \times 20$  to detect small objects (stars).

For the training of the stars detector, various images with different spot sizes are used from the reconstructed DAE dataset. 480 images are used for training and 26 images for validation. The standard YOLOv5 models are trained, such as YOLOv5 n, s, m, and l. Then, the proposed model was trained with the same training parameters (epochs, batch size, learning rate, optimizer, etc.). The models were fine-tuned with an Adam optimizer. A comparative study was performed to evaluate our architecture in terms of accuracy, inference time, and architecture complexity with the standard YOLOv5 models.

Once the model is trained, this trained YOLO model is used for inference. The stars bounding boxes are extracted to compute the centroid of each star within the box. Thus, the Center Of Gravity (COG) method is used. The COG method calculates the coordinates and intensity of each detected star in the image. The output of the algorithm is a set of values, X, Y, and I, for each star.

$$(xc, yc) = \left( \frac{\sum_{ij} X_{ij} * I_{ij}}{\sum_{ij} I_{ij}}, \frac{\sum_{ij} Y_{ij} * I_{ij}}{\sum_{ij} I_{ij}} \right) \text{ Eq.(2)}$$

X corresponds to the horizontal location of the star and has a value between 0 and 416. Y is the vertical location of the stars and has a value between 0 and 416. (I) is the pixel intensity of the star and has a value between 0 and 255.

### III. EXPERIMENTAL RESULTS

#### A. Experiments

##### a. Denoising Auto-Encoder (DAE)

First, different models of noise with different levels are added to clean images such as Gaussian noise, salt & pepper noise, shot noise, and dark noise. Then, different denoising techniques are applied to these images to measure the relative performance of our method. Fig.9 shows some examples of added noise: Gaussian noise with mean = 0 and  $\sigma = 20$  (PSNR = 16.13 dB), salt and pepper noise (PSNR = 16.48 dB), shot noise (PSNR = 16.0 dB) and dark noise (PSNR = 16.19 dB).

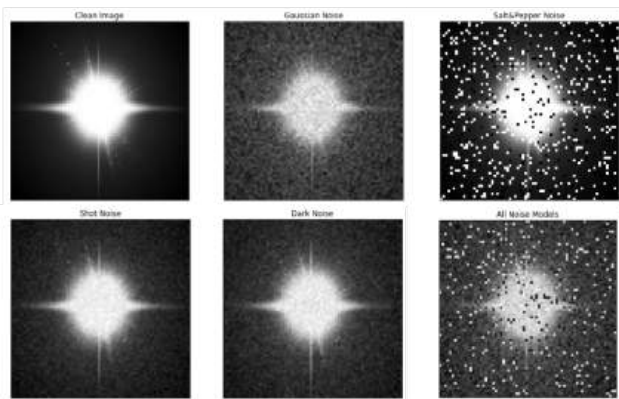


Fig.9: Different noise models for star images

Once the images are noisy, traditional filtering methods are applied using the OpenCV library to reconstruct the corrupted

star. These methods are the Gaussian filter, mean filter, median filter, Wiener filter, and Bilateral filter. For each filter type, the optimal window size was determined experimentally (by trying different window sizes) to ensure the best results. The image quality is evaluated by the signal-to-noise ratio (PSNR):

$$\text{PSNR} = -10 \log_{10} \frac{\text{MSE}}{I^2} ; I \text{ is the maximum}$$

pixel value.

Where:

$$\text{MSE} = \sum_{m=1}^M \sum_{n=1}^N [I_{\text{original}}(\mathbf{m}, \mathbf{n}) - I_{\text{filtered}}(\mathbf{m}, \mathbf{n})]^2$$

$I_{\text{original}}$  and  $I_{\text{filtered}}$  represent, respectively, the matrix (pixel values) of the original image and the matrix of the filtered image. M and N are, respectively, the number of rows of pixels and the number of columns of pixels.

The Centroid Estimation Error (CEE) is used to evaluate the centroid error using the formula:

$$\text{CEE} = \sqrt{(x_e - x_c)^2 + (y_e - y_c)^2}$$

where  $(x_e, y_e)$  is the estimated centroid and  $(x_c, y_c)$  is the actual centroid. Effectively, the CEE measures the distances of the estimated centroid from the actual position of the star. Thus, the root mean square error (RMSE) of the stars in the image is computed using the formula.

$$\text{RMSE} = \frac{1}{2} \times \sqrt{\frac{(x_e - x_c)^2}{n} + \frac{(y_e - y_c)^2}{n}}$$

where n is the number of detected stars in the image.

The best solution is the filter that resists all types of noise with higher PSNR and low CEE.

##### b. Star detection

For the Star detection experiments, the five standard YOLOv5 models (extra-large, large, medium, small, and nano architectures) are evaluated and compared to the modified lightweight architecture. The inference time is measured using a batch size of 32 testing images and running on Nvidia Tesla T4 GPU.

#### B. Results

##### a. Denoising Auto-Encoder (DAE)

To evaluate the performance of each filtering technique, the PSNR, and the centroiding error is used as evaluation metrics. Six conventional filters were applied to the input image to reduce the different types of noise.

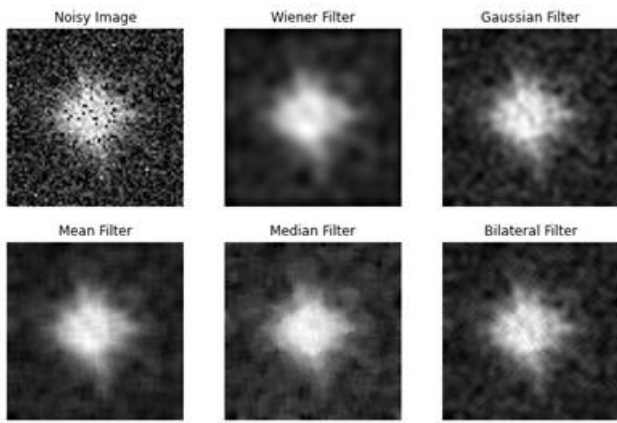


Fig.10: Filtering techniques results on all noise models

Fig.10 presented the results of different 5-by-5 filter types such as Gaussian Filter, Mean Filter, Median Filter, Bilateral Filter, and Wiener Filter. It can be noticed that the noise tends to be eliminated with each type of filter, but some details like edges become blurred and the background noise is still present. It is difficult to determine the best technique to reduce noise from images. However, PSNR and centroiding error is used to evaluate the results.

The DAE-trained model is applied against different types of noise that affect the star image to evaluate the efficiency and robustness of the model.

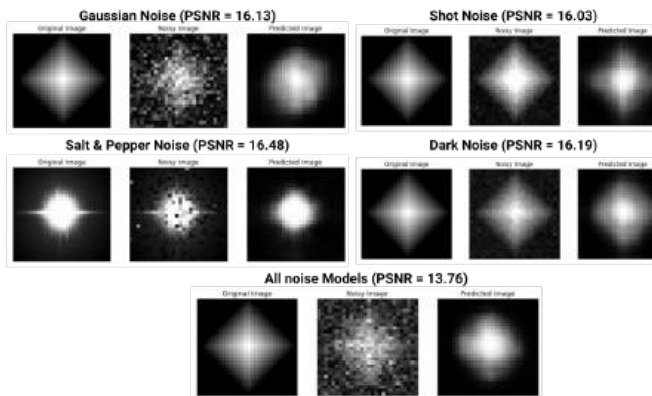


Fig.11: DAE output - Reconstructed star

Fig.11 shows how DAE resists any noise type that can affect the star image. It can be noticed that DAE reconstructs more luminance pixels (pixel value  $\approx 255$ ) than low luminance pixels (pixel value  $\ll 255$ ) when the noise level is high (low PSNR). Thus, the luminance of the star pixels is strongly related to the centroid accuracy.

To ensure that the DAE model distinguishes between the noise pixels and starspot size, a real image affected by some noise models (Gaussian, salt & pepper, and shot noise) is used. The 3D energy distribution of this image shows how the noise is spread over the whole image and makes it difficult to distinguish between the stars and the noise of the background. However, the 3D distribution of the image after the denoising

process shows that the image noise has been reduced and the light peaks caused by the pepper noise were removed.

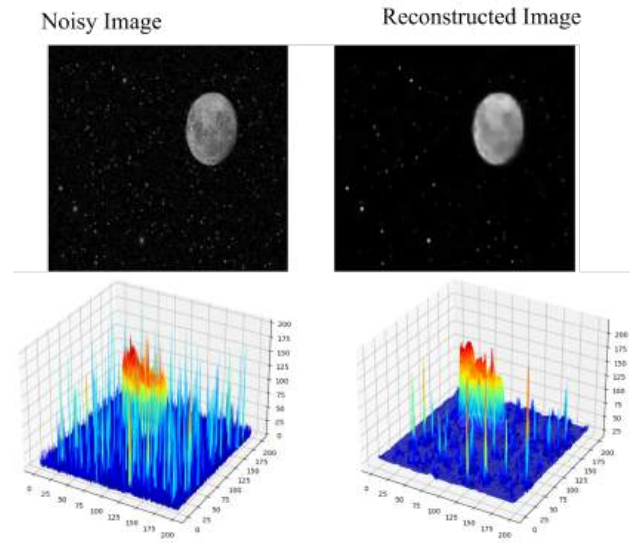


Fig.12: 3D energy Distribution

The PSNR has been computed for different filter techniques to evaluate the result of each technique against each type of noise. Fig.13 shows that the PSNR of DAE is much better (PSNR  $\approx 70$ dB) than the traditional techniques (PSNR  $\approx 30$ dB) in all noise cases, which ensures a high-quality image as output. Salt and pepper noise presents a critical noise in star detection due to the small white features caused by this type of noise (Fig.12). That causes false star detection, thus the result of the DAE against the salt and pepper noise (Fig.12 and Fig.13) confirms that the noise spots will be removed before the detection process.

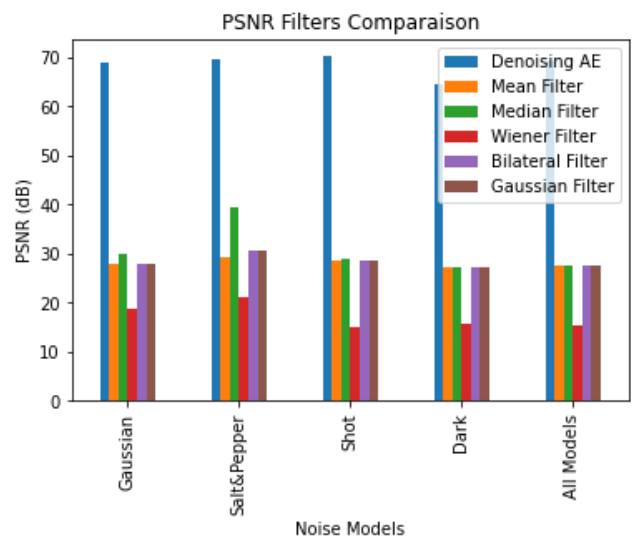


Fig.13: Peak Signal-to-Noise Ratio of Filter Techniques

The experiments (Fig.13 and Fig.14) make it clear that DAE is an effective technique to restore corrupted images with high quality (PSNR $>40$ dB) compared to the previous

filtering techniques. The centroiding is also used as a second metric to evaluate the filtering techniques and robustness against noise by computing the centroid error between the original and reconstructed images.

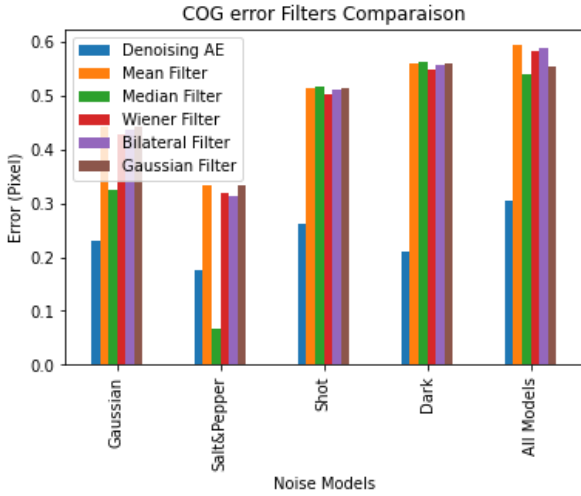


Fig.14: COG error of filter techniques

Fig.14 shows that the COG error of DAE is decreased by 0.3 pixels as compared to other filtering methods. For the salt and pepper noise, the median filter is still the best solution [37]. However, this filter is not a good solution to reduce the other noise types. In a realistic application with combined noise models, our solution outperforms the other filtering techniques. pepper noise (Fig.12 and Fig.13) confirms that the noise spots will be removed before the detection process.

### b. Star detection

For star detection evaluation, comparative studies between the proposed architecture and the standard YOLOv5 architectures are presented (Table 1).

MODELS	mAP@0.5	mAP@0.5:0.95	GFLOPs	Weights size (MB)	Inference @batch size32 (ms)
YOLOv5X	0.61	0.158	203.8	173	26.8
YOLOv5L	0.601	0.167	107.6	92.7	15.9
YOLOv5M	0.732	0.212	47.9	42.1	9.1
YOLOv5S	0.686	0.198	15.8	14.3	4.9
YOLOv5N	0.737	0.218	4.1	3.7	4.4
PROPOSED	0.682	0.211	0.6	0.3	1.9

TABLE 1: COMPARISON OF THE YOLOv5 MODELS

From the table above, it can be noticed that the models with less complexity architecture (YOLOv5m, YOLOv5s, and YOLOv5n) achieve better accuracy (mAP@0.5≈73%, mAP@0.5:0.95≈21) than the largest architectures (YOLOv5l and YOLOv5x). Therefore, the modified model (proposed) achieves practically the same accuracy as the small YOLOv5 architecture with less architectural complexity. In addition, the GFLOPs of the modified architecture is more than 3x decreased compared to the YOLOv5 nanoarchitecture. Furthermore, the number of layers is reduced (67 layers have been removed) and the weight of the model is reduced by 10 times compared to the nanoarchitecture, which clearly facilitates deployment on the embedded device.

For inference, a batch size of 32 is used to evaluate the mode. The time inference of the modified YOLOv5n model (1.9ms) is reduced by 2.5 ms compared to the nano YOLOv5 model (4.4ms) which is better for real-time applications.

## IV. DISCUSSION

To remove noise from images, several methods exist. In this paper, a CNN technique was proposed to resist several most prevalent noise types and provide high image quality for star trackers. The experiments showed how the DAE is useful to remove several types and levels of noise which ensures more performant star detection with fewer false stars as well as more accurate centroids, whereas the COG method is recommended with a low noise level.

The results of star detection parts confirmed that the proposed YOLO architecture provides high performance compared to other state-of-the-art techniques. In terms of latency, the YOLO family is superior compared to the traditional methods. Although all of the YOLOv5 models achieved state-of-the-art accuracy results, they were time-consuming due to the complexity of the architecture and a large number of parameters. Therefore, the proposed model mitigates the trade-off between high accuracy and low complexity, achieving both. This makes our model applicable for real-time star-tracking tasks. The experiments confirm that the proposed model achieved high performance in extracting all stars in the images including faint stars. The fast centroiding technique (COG) and lightweight object detection will speed up the detection as well as centroid computation by using bounding boxes. Generally, the use of the COG method leads to a large error in wavefront reconstruction due to the noise of the background, however, this negative is limited when the background noise is filtered by the DAE.

## V. CONCLUSION AND FUTURE WORK

Applying deep learning algorithms in space applications is still an active topic of research. The trade-off between high accuracy and low hardware computation is required for real-time applications. Our main focus was to implement advanced deep-learning algorithms for star trackers to solve some common problems such as noise removal. The results of our DAE confirm the ability of the method to remove noise and reconstruct the corrupted star without any major loss of information. This achievement ensures high image quality and, consequently, accurate centroid calculation for a precise attitude determination. Denoising is one of the main tasks of

computer vision, not only in space applications but in most fields. Our star detector based on a modified YOLOv5 architecture reduces the computational complexity concerning YOLOv5 standard models and thus is needed to deploy on edge devices. The bounding boxes of YOLO were also needed for centroid computation to ensure the accuracy of the centroiding by computing the white pixels within each bounding box using the fastest method, COG. The use of an efficient denoising technique and an accurate object detector ensures the high accuracy of the centroid calculation and, hence, the accuracy of the attitude determination, which is the aim of the star tracker sensor.

To reach the aim of the work in developing efficient and lightweight deep learning engines for a real-time star tracking system, the next challenge will be the optimization of the pipeline using Intel Software's optimization tools (e.g. OpenVINO) and Intel Movidius NCS for model inference and hardware deployment.

#### REFERENCES

- [1] Enright, John, Doug Sinclair, Cordell Grant, Geoff McVittie, and Tom Dzamba. "Towards star tracker only attitude estimation." (2010).
- [2] Lindh, Marcus. "Development and Implementation of Star Tracker Electronics." (2014).
- [3] Boyat, Ajay Kumar, and Brijendra Kumar Joshi. "A review paper: noise models in digital image processing." arXiv preprint arXiv:1505.03489 (2015).
- [4] Caixia Zheng, Jesus Pulido, Paul Thorman, Bernd Hamann, An improved method for object detection in astronomical images, Monthly Notices of the Royal Astronomical Society, Volume 451, Issue 4, 21 August 2015, Pages 4445–4459, <https://doi.org/10.1093/mnras/stv1237>
- [5] Desai, Bhishman & Kushwaha, Utkarsh & Jha, Shivam. (2020). Image Filtering -Techniques, Algorithm, and Applications. Applied GIS. 7. 101.
- [6] Knutson, Matthew Walter. "Fast star tracker centroid algorithm for high performance CubeSat with air bearing validation." PhD diss., Massachusetts Institute of Technology, 2012.
- [7] Caixia Zheng, Jesus Pulido, Paul Thorman, Bernd Hamann, An improved method for object detection in astronomical images, Monthly Notices of the Royal Astronomical Society, Volume 451, Issue 4, 21 August 2015, Pages 4445–4459, <https://doi.org/10.1093/mnras/stv1237>
- [8] L. Kazemi, J. Enright and T. Dzamba, "Improving star tracker centroiding performance in dynamic imaging conditions," 2015 IEEE Aerospace Conference, Big Sky, MT, USA, 2015, pp. 1-8, doi: 10.1109/AERO.2015.7119226.
- [9] P. Roy, S. Dutta, N. Dey, G. Dey, S. Chakraborty and R. Ray, "Adaptive thresholding: A comparative study," 2014 International Conference on Control, Instrumentation, Communication and Computational Technologies (ICCCICT), Kanyakumari, India, 2014, pp. 1182-1186, doi: 10.1109/ICCCICT.2014.6993140.
- [10] Yousefi, Jamileh. (2015). Image Binarization using Otsu Thresholding Algorithm. 10.13140/RG.2.1.4758.9284.
- [11] Wen-Hsiang Tsai, Moment-preserving thresholding: A new approach, Computer Vision, Graphics, and Image Processing, Volume 29, Issue 3, 1985, Pages 377-393, ISSN 0734-189X, [https://doi.org/10.1016/0734-189X\(85\)90133-1](https://doi.org/10.1016/0734-189X(85)90133-1)
- [12] Dikmen, Serkan. "Development of star tracker attitude and position determination system for spacecraft maneuvering and docking facility." (2016).
- [13] Ting Sun, Fei Xing, Zheng You, and Minsong Wei, "Motion-blurred star acquisition method of the star tracker under high dynamic conditions," Opt. Express 21, 20096-20110 (2013)
- [14] Patidar, Pawan, Manoj Gupta, Sumit Srivastava, and Ashok Kumar Nagawat. "Image de-noising by various filters for different noise." International journal of computer applications 9, no. 4 (2010): 45-50.
- [15] Girshick, Ross, Jeff Donahue, Trevor Darrell, and Jitendra Malik. "Rich feature hierarchies for accurate object detection and semantic segmentation." In Proceedings of the IEEE conference on computer vision and pattern recognition, pp. 580-587. 2014.
- [16] Girshick, Ross. "Fast r-cnn." In Proceedings of the IEEE international conference on computer vision, pp. 1440-1448. 2015.
- [17] Ren, Shaoqing, Kaiming He, Ross Girshick, and Jian Sun. "Faster r-cnn: Towards real-time object detection with region proposal networks." Advances in neural information processing systems 28 (2015).
- [18] Liu, Wei, Dragomir Anguelov, Dumitru Erhan, Christian Szegedy, Scott Reed, Cheng-Yang Fu, and Alexander C. Berg. "Ssd: Single shot multibox detector." In Computer Vision—ECCV 2016: 14th European Conference, Amsterdam, The Netherlands, October 11–14, 2016, Proceedings, Part I 14, pp. 21-37. Springer International Publishing, 2016.
- [19] J. Redmon, S. Divvala, R. Girshick and A. Farhadi, "You Only Look Once: Unified, Real-Time Object Detection," 2016 IEEE Conference on Computer Vision and Pattern Recognition (CVPR), Las Vegas, NV, USA, 2016, pp. 779-788, doi: 10.1109/CVPR.2016.91.
- [20] Delabie, Tjorven, Joris De Schutter, and Bart Vandenbussche. "An accurate and efficient gaussian fit centroiding algorithm for star trackers." The Journal of the Astronautical Sciences 61 (2014): 60-84.
- [21] Vincent, Pascal, Hugo Larochelle, Yoshua Bengio, and Pierre-Antoine Manzagol. "Extracting and composing robust features with denoising autoencoders." In Proceedings of the 25th international conference on Machine learning, pp. 1096-1103. 2008.
- [22] Bank, Dor, Noam Koenigstein, and Raja Giryes. "Autoencoders." arXiv preprint arXiv:2003.05991 (2020).
- [23] Redmon, Joseph, Santosh Divvala, Ross Girshick, and Ali Farhadi. "You only look once: Unified, real-time object detection." In Proceedings of the IEEE conference on computer vision and pattern recognition, pp. 779-788. 2016.
- [24] Wang, Chien-Yao, Hong-Yuan Mark Liao, Yueh-Hua Wu, Ping-Yang Chen, Jun-Wei Hsieh, and I-Hau Yeh. "CSPNet: A new backbone that can enhance learning capability of CNN." In Proceedings of the IEEE/CVF conference on computer vision and pattern recognition workshops, pp. 390-391. 2020.
- [25] He, Kaiming, Xiangyu Zhang, Shaoqing Ren, and Jian Sun. "Spatial pyramid pooling in deep convolutional networks for visual recognition." IEEE transactions on pattern analysis and machine intelligence 37, no. 9 (2015): 1904-1916.
- [26] Huang, Zhanchao, Jianlin Wang, Xuesong Fu, Tao Yu, Yongqi Guo, and Rutong Wang. "DC-SPP-YOLO: Dense connection and spatial pyramid pooling based YOLO for object detection." Information Sciences 522 (2020): 241-258.

# Performance Assessment of GNSS systems to support Remote Sensing in Africa.

Herbert NGAYA<sup>1</sup>, Alou Aicha<sup>2</sup>, Alex Wanda<sup>3</sup>,

*SatNav Africa –JPO*

*aicha.alou@satnav-africa.com, alex.wanda@satnav-africa.com, herbert.ngaya@satnav-africa.com*

**Keywords:** GNSS, Remote Sensing, Reflectometry

Global Navigation Satellite Systems have been developed to provide Positioning, Navigation and Timing services. By GNSS positioning a multipath signal is often considered an undesirable phenomenon that needs to be suppressed. A reflected GNSS signal (also known as multipath- or scattered signal) is regarded as an error source that lowers the positioning accuracy. But these scattered signals can be used in many remote sensing applications. The exploitation of Global Navigation Satellite Systems signals for Remote Sensing (GNSS-RS) provides an innovative, cost-effective, and versatile tool for Earth system observation

Remote sensing when using GNSS makes use three techniques that include ground-based sounding techniques, radio occultation (GNSS-RO) and reflectometry (GNSS-R). This paper shall focus on GNSS-R, which is a technique aimed at collecting direct and reflected signals from a GNSS transmitter and interpret the data as information of a surface state.

When energy like microwave radiation interacts with substances like soil and vegetation, some of it is absorbed, some passes through, and some is reflected. The amount that is reflected depends upon the dielectric constant and the angle of the incoming radiation.

The global coverage from many dozens of transmitting satellites in multiple constellations and wide-bandwidth ranging signals, make the use of GNSS-R techniques attractive as they offer low cost means for remote sensing.

The accuracy of the system depends much on the facility set-up. Since one of the GNSS-R's antennas receives only the reflected signals, the ability of the receiver to perform SV locking becomes important. On the African continent there is need to assess the quality of GNSS signals received so as to have an insight into the potential of GNSS Reflectometry.

In this paper, we shall analyze the quality indicator, i.e., the SNR of the direct and reflected signals from different GNSS constellations received on the continent. The main objective of this study is to characterize if the direct and reflected signal from GNSS systems, can be received with enough SNR.

## Ionospheric Plasma Irregularities and their Impact on GNSS Services

Wojciech J. Miloch<sup>1\*</sup>, and 4DSpace team<sup>1</sup>

<sup>1</sup>*Department of Physics, University of Oslo, Norway*

[w.j.miloch@fys.uio.no](mailto:w.j.miloch@fys.uio.no)

**Keywords:** Ionosphere, GNSS, GPS, Irregularities, Scintillations, Space Weather

The ionosphere is the uppermost part of the atmosphere that is partially ionised, thus being in a plasma state. Its dynamics is coupled to processes in the magnetosphere and solar wind, and it is a part of a space weather system. Ionospheric plasmas are often subject to instabilities and turbulence, which consequently lead to plasma irregularities at various scales. At high geomagnetic latitudes, plasma irregularities can be due to a multitude of phenomena that give rise to plasma structuring, such as the auroral particle precipitation or patches of enhanced plasma density moving in the polar cap. At low latitudes, structuring is dominant in the post-midnight equatorial sector and can be associated with the Equatorial Spread F, which includes plasma density depletions often referred to as bubbles. During increased geomagnetic activity, plasma structures often propagate towards mid-latitudes. Ionospheric plasma irregularities can influence the propagation of radio signals, leading to scintillations in phase and amplitude of the received wave. They can degrade communication or positioning with the Global Navigation Satellite Systems (GNSS), and their understanding is an important aspect for developing space weather models and building the capability of predicting and mitigating severe space weather effects.

Low-Earth-Orbiting (LEO) satellites can provide global insight into plasma structuring by in-situ measurements. An example is the European Space Agency's Swarm mission, which is a constellation of three satellites in slowly drifting polar orbits. We have developed a Swarm data product Ionospheric Plasma Irregularities (IPIR), which allows for quantifying and characterizing the plasma structuring along the whole orbits of the satellites [1]. IPIR combines complementary datasets from the Swarm satellites, i.e., the electron density from the electric field instrument, the GPS data from the onboard GPS receiver, and the magnetic data from the vector field magnetometer. In this work, we present the IPIR data product and how it can be used to characterize the whole ionosphere. We also discuss different aspects of the plasma structuring based on the Swarm data, with a focus on the African sector, and how the IPIR dataset, and thus data from LEO satellites, can be related to the ground-based measurements of ionospheric scintillations and contribute to the development of space weather models.

[1] Y. Jin, D. Kotova, Ch. Xiong, S. M. Brask, L.B.N. Clausen, G. Kervalishvili, C. Stolle, W.J. Miloch, Ionospheric Plasma Irregularities - IPIR - data product based on data from the Swarm satellites, *J. Geophys. Res.* 127, e2021JA030183, <https://doi.org/10.1029/2021JA030183> (2022).



# 2<sup>nd</sup> Conference on SPACE STAR

Science, Technology, Applications & Regulation

October 18-20, 2023, Sousse, TUNISIA

## Design and Fabrication of a Controllable Environment for CubeSat Attitude Testing

Samer Lahouar<sup>1,3\*</sup>, Mounir Mansour<sup>2,3</sup>

<sup>1</sup>*Center for Research on Microelectronics and Nanotechnology, Sousse, Tunisia;*

<sup>2</sup>*Military academy of Fondouk Jedid, Tunisia;*

<sup>3</sup>*Microelectronics and Instrumentation Laboratory, Faculty of Sciences of Monastir, University of Monastir, Tunisia.*

[samer.lahouar@crmn.rnrt.tn](mailto:samer.lahouar@crmn.rnrt.tn)

**Keywords:** CubeSat, ADCS, Helmholtz Cage.

The work presented in this paper is accomplished in the framework of the FACT project, which is coordinated by the Center for Research on Microelectronics and Nanotechnology (CRMN) of Sousse and involves other national research and industrial partners. One of the objectives of the FACT project is to train researchers and students from Tunisian universities on space technologies, and specifically CubeSat development.

A CubeSat is a standard form of nanosatellite composed of many subsystems that have each a specific function. The different subsystems of the CubeSat interact together to ensure the success of its mission. One crucial subsystem of a CubeSat is the Attitude Determination and Control Subsystem (ADCS), which provides stability and pointing accuracy of the CubeSat and its other components, such as the payload or the antennas.

Depending on the CubeSat mission, the ADCS can use different techniques to provide the required stability and pointing accuracy. For one-unit CubeSats (1U), a magnetic based ADCS system is usually utilized since it has a relatively small size and low power consumption. This system uses earth's magnetic field to stabilize the CubeSat after its deployment in space (detumbling procedure). Moreover, the system also uses earth's magnetic field to point the CubeSat in the required direction.

To test the magnetic based ADCS system and evaluate its performance in the lab, a magnetic field that simulates earth's magnetic field, as measured by the CubeSat in orbit, must be generated and applied to the system. The generated magnetic field should be controlled both in amplitude and direction in a manner that mimics changes in earth's magnetic field seen by the CubeSat while orbiting the earth. As found in literature, Helmholtz coils assembled into a Helmholtz cage can provide the required controllable magnetic field.

In this context, we present in this paper the design of a Helmholtz cage that can be used to evaluate the performance of a 1U-CubeSat-ADCS system. First, the paper discusses the requirements needed to obtain a magnetic field variation inside the cage in the range of earth's magnetic field. Then, the mechanical design of the coils (i.e., size, number of turns, and position) making the cage is detailed. To accurately control the generated magnetic field's amplitude and direction, a control system is developed along with a graphical user interface. Using a feedback loop, the control system allows to automatically power the coils to obtain the magnetic field set by the user. Moreover, using a specially designed algorithm, the Helmholtz cage can be used to automatically calibrate a magnetometer and remove the hard iron and soft iron effects that can distort the measured fields.

To evaluate the performance of the Helmholtz cage, testing results are presented. The tests show that the Helmholtz cage can generate a constant magnetic field within a space at its center larger than the size of the CubeSat. Moreover, the generated fields can be accurately controlled to simulate the variations of earth's magnetic field in orbit.



# 2<sup>nd</sup> Conference on SPACE STAR

Science, Technology, Applications & Regulation

October 18-20, 2023, Sousse, TUNISIA

## Study and Implementation of CubeSat Attitude Control Based on Magnetorquer

M. Mansour<sup>1,3\*</sup>, S. Lahouar<sup>2,3</sup>

<sup>1</sup> *Military Academy, Fondouk Jédid, Tunisia;*

<sup>2</sup> *Center for Research on Microelectronics and Nanotechnology, Sousse, Tunisia;*

<sup>3</sup> *Microelectronics and Instrumentation Laboratory, Faculty of Sciences of Monastir, University of Monastir, Tunisia.*

[mounir.mansour@issatso.u-sousse.tn](mailto:mounir.mansour@issatso.u-sousse.tn)

**Keywords:** CubeSat, ADCS, detumbling.

The attitude of a satellite refers to its orientation in space. Controlling this attitude is very important since it provides stability and pointing accuracy of the payloads and antennas, which are critical parameters for the satellite's mission success. In a satellite, this operation is performed by the Attitude Determination and Control System (ADCS).

The study and development of a complete ADCS system of a CubeSat is conducted in the framework of the FACT project, which is coordinated by the Center for Research on Microelectronics and Nanotechnology (CRMN) of Sousse and involves other research and industrial partners. The objective of the FACT project is to train researchers and students from Tunisian universities on space technologies.

Several modules onboard the CubeSat can benefit from attitude control and the ability to point the satellite accurately:

- A camera payload needs pointing accuracy and slow angular velocity to take good pictures.
- The communication between the CubeSat and a ground station can be optimized, if the satellite antenna tracks the ground station.
- Power generated from the solar panels can be optimized, by maximizing the surface area of the solar panels pointing towards the Sun.

In a CubeSat, the ADCS can also be used in detumbling, which is a very important phase to stabilize the satellite. In fact, the deployment of the CubeSat in space, from a Poly-PicoSatellite Orbital Deployer (P-POD) for example, will cause it to tumble around its axes of inertia.

In this context, we present a study and development of a control and command system based on the B-Dot algorithm. This command will be used to ensure the de-tumbling sequence after the satellite deployment. Simulations have been first conducted, using the Matlab-Simulink environment, to study the command law. Then implementation of this command was done, on a CubeSat prototype. The control system uses two magnetic actuators (magnetorquers), also designed and built within the CRMN, as part of the same project.

Tests are done using a testbed platform that allows to simulate the operation of an ADCS module. The testbed is based on a Helmholtz cage that permits creating a test environment in which the magnetic field produced can be controlled. The testbed and the CubeSat prototype have also been designed and built within the CRMN of Sousse as part of the FACT project.

The design of the control and command system and the preliminary test results are also presented in this paper.

## Miniaturized symmetric double E-shaped microstrip patch antenna for CubeSat Communication

Nozha ZALFANI<sup>1</sup>, Samer Lahouar<sup>12\*</sup>, Kamel Besbes<sup>12\*</sup>

<sup>1</sup>*Microelectronics & Instrumentation Lab, Faculty of Sciences of Monastir, University of Monastir, Tunisia;* <sup>2</sup>*Centre for Research on Microelectronic & Nanotechnology (CRMN), Sousse Technopole, Tunisia*

[nozha.zalfani@gmail.com](mailto:nozha.zalfani@gmail.com), [samer.lahouar@crmn.rnrt.tn](mailto:samer.lahouar@crmn.rnrt.tn), [kamel.besbes@fsm.rnu.tn](mailto:kamel.besbes@fsm.rnu.tn)

**Keywords:** E-shaped microstrip patch antenna, UHF communication, CubeSat, Long-range (LoRa), Internet of things (IoT)

IoT refers to the network connectivity of numerous objects. These devices frequently run on batteries and require an extensive battery backup. These systems need a technology that uses less energy and has an extensive range. These requirements for an embedded device that runs on batteries meet the criteria of LoRa technology. LoRa requires the use of satellite networks in order to achieve global IoT coverage. The deployment of picosatellites such as CubeSats can provide a wide coverage area with a long communication range. Similar to traditional satellites, they are viable and robust yet cost less, use less power, and allow for quick development. However, because of its compactness, the circuitry and components must be smaller and more power-efficient. Their antennas, which must be lightweight, compact, and small in size.

This work presents the design of a Miniaturized symmetric double E-shaped microstrip patch antenna for CubeSat Communication working at a range of frequency between 470 MHz to 1.2 GHz. The structure of this proposed antenna has a low profile and a small size of 31 \* 62 \* 1.635 mm<sup>3</sup>. The antenna geometry fits on any CubeSat standard structure and ensures a gain of 1.6 dB.

Abstract proposal for the STAR conference (specific section devoted to the H2020-Marie Skłodowska Curie Action-RISE ACCWA project, on the 19th of October)

## **Classification of Irrigation Systems at Field Level from Remotely Sensed Soil Moisture and Actual Evapotranspiration TimeSeries**

Paolini Giovanni <sup>(1) (\*)</sup>, Escorihuela Maria Jose <sup>(1)</sup>, Merlin Olivier <sup>(2)</sup>, Pamies-Sans Magí <sup>(3)</sup>, Bellvert Joaquim <sup>(3)</sup>

(1) isardSAT, Parc Tecnologic Barcelona Activa, Carrer de Marie Curie, 8, 08042, Catalunya, Spain

(2) CESBIO (Centre d'Études Spatiales de la Biosphère), University of Toulouse, CNES/CNRS/INRAE/IRD/UPS, 18 Avenue Edouard Belin, Toulouse, 31401, France

(3) Efficient Use of Water in Agriculture Program, Institut de Recerca i Tecnologia Agroalimentaries (IRTA), Fruitcentre, Parc Científic i Tecnològic Agroalimentari (PCiTAL), Lleida, 25003, Catalunya, Spain

(\*) [giovanni.paolini@isardsat.cat](mailto:giovanni.paolini@isardsat.cat)

**keywords:** irrigation systems, actual evapotranspiration, soil moisture, time-series classification, artificial intelligence

This study proposes a novel methodology for classifying irrigation systems at field scale, in order to address the lack of such maps at high resolution from remotely sensed data. This information has critical scientific value since detailed information on irrigation practices greatly improves the understanding of human activities in the water cycle. In particular, precise knowledge of different irrigation systems is needed in order to correctly model the anthropogenic impact in various land surface models. Additionally, these maps are also useful for administrative purposes, to estimate the percentage of different irrigation systems, monitor changes in irrigation practices and consequently encourage more sustainable use of freshwater resources. The hypothesis of this study is that time-series of two main hydrological variables, Actual Evapotranspiration (ETa) and Soil Moisture (SM) at high resolution (20 m) show variations directly related to the different irrigation systems used. Three different Artificial Intelligence (AI) models for time-series classification were employed and compared for this specific task: two classical machine learning algorithms, Time-Series Forest and Rocket, and one deep learning model, ResNET. In order to train these models, an extensive field campaign was performed in 2020 in an intensively cultivated region in Catalunya, Spain. Data for more than 300 fields were collected, from different crop types and labeled by four different classes: flood, sprinkler, drip, and not irrigation. The classification was performed using time-series from three different years in order to train the models with a more general and robust dataset, independent from specific meteorological conditions of a single year. Initially, we demonstrated how irrigation systems are correctly classified from ETa and SM regardless of the crop type used: AI models were trained separately for each crop type and results were aggregated together and compared with a general AI model trained with all crop types. Secondly, tests were performed to identify the most suitable AI model and also to identify the most suitable set of variables for the classification, among ETa, SM, but also Leaf Area Index, Crop Stress Coefficient, Normalized Difference Vegetation Index, and Land Surface Temperature. Results showed how combining ETa and SM produced the best classification results in terms of accuracy of around 90 %, when used with ResNET. As a result, it was possible to create annual maps of irrigation systems for the considered study area, which showed a general trend towards modern irrigation systems such as drip and sprinklers.

## Exploring Agricultural Drought Indices for Cereal Yield Prediction Assessment in Semi-Arid Regions

Manel Khlif<sup>1,\*</sup>, Maria José Escorihuela<sup>2</sup>, Aicha Chahbi Bellakanji<sup>1</sup>, Giovanni Paolini<sup>2</sup> and Zohra Lili Chabaane<sup>1</sup>

<sup>1</sup> *University of Carthage, National Agronomic Institute of Tunisia, LR GREEN-TEAM. 43 Avenue Charles Nicolle, Tunis 1082, Tunisia;* <sup>2</sup> *isardSAT, Technological Park, Marie Curie, 8-14, 08042, Barcelona, Catalonia*  
[manel.khlif@inat.u-carthage.tn](mailto:manel.khlif@inat.u-carthage.tn)

**Keywords:** Agriculture Drought, Cereal yield, Remote sensing

The increasing impact of climate change has led to a rise in the frequency and severity of drought events, posing a serious threat to agriculture and food security, which rely heavily on cereals. This phenomenon is widespread in Mediterranean countries, where increasing agricultural water demand and decreasing water resources are aggravating water stress situations and impacting cereal production.

This study aimed to achieve two objectives: 1) to analyze the potential of different agriculture drought indices for identifying drought periods, and 2) to select the most informative drought index and period for predicting cereal yield. Two Mediterranean regions, namely Lleida in Catalonia and Kairouan in Tunisia, were studied in view of their similar semi-arid climates but different agricultural practices.

Four drought indices, namely the Soil Moisture Anomaly Index (SMAI), Vegetation Anomaly Index (VAI), Evapotranspiration Anomaly Index (EAI), and Inverse Temperature Anomaly Index (ITAI) were calculated using SMOS DISPATCH SM, MOD13Q1, MOD16A2, and MOD11A2 remote sensing data, respectively. Drought periods were identified from September 2010 to August 2022 based on the aforementioned drought indices. Subsequently, a correlation study between drought indices and wheat and barley yields was conducted to determine the most informative index and month for yield prediction.

In the rainfed cereal area of Lleida, the strongest correlation was found between EAI and VAI with barley yield (0.91 and 0.83 respectively) at the time of cereal maturity in June. For wheat, the strongest correlation was found between EAI and VAI (0.76 and 0.72 respectively) at the time of cereal maturity in July. However, SMAI showed the best performance as an earlier indicator in March (roughly three months before harvest) with the highest correlation with barley and wheat yield (0.7 and 0.63 respectively) and the lowest standard deviation. For the irrigated cereal zone of Kairouan, the strongest correlation (0.9) and the lowest standard deviation are found between EAI and cereal yield in April (this is one or two months before harvest). In terms of advanced prediction, VAI shows a high correlation in March (0.79) while SMAI shows a slightly lower correlation in February (0.67) but with a lower standard deviation.

The obtained results highlight the importance of SMAI as a crucial indicator for the early estimation of cereal yields. These findings offer valuable insights for decision-making processes related to food security through early yield prediction and the implementation of more effective water management strategies.